

Candidate Anode Materials for Iron Production by Molten Oxide Electrolysis

by

James D. Paramore

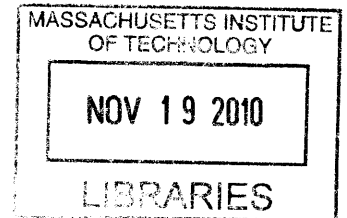
B.S. Metallurgical Engineering
University of Utah, 2007

Submitted to the Department of Materials Science and Engineering
in Partial Fulfillment of the Requirements for the Degree of
Master of Science in Materials Science and Engineering

at the

Massachusetts Institute of Technology

September 2010



©2010 Massachusetts Institute of Technology.
All rights reserved.

ARCHIVES

Signature of Author: _____

A handwritten signature in black ink, appearing to read "James D. Paramore".

Department of Materials Science and Engineering
August 13, 2010

Certified by: _____

A handwritten signature in black ink, appearing to read "Donald R. Sadoway".

Donald R. Sadoway
John F. Elliot Professor of Materials Chemistry
Thesis Supervisor

Accepted by: _____

Christopher Schuh
Chair, Departmental Committee on Graduate Students

Candidate Anode Materials for Iron Production by Molten Oxide Electrolysis

by

James D. Paramore

Submitted to the Department of Materials Science and Engineering
on August 13, 2010 in Partial Fulfillment of the
Requirements for the Degree of Master of Science in
Materials Science and Engineering

ABSTRACT

Molten oxide electrolysis (MOE) has been identified by the American Iron and Steel Institute (AISI) as one of four possible breakthrough technologies to alleviate the environmental impact of iron and steel production. This process has also been identified by the National Aeronautics and Space Administration (NASA) as a means to produce oxygen gas, as well as iron and silicon raw materials on the Moon. MOE produces iron by electrolysis of an iron oxide containing electrolyte. The electrolysis results in the production of pure iron metal at the cathode and pure oxygen gas at the anode. Because of the low vapor pressure of the electrolyte at temperatures above 1538°C, MOE can be performed above the melting temperature of iron. The production of liquid metal, ready for continuous casting, is a prerequisite for any industrial-scale extractive metallurgical process. Therefore, if an inert anode can be identified, MOE could provide an industrial process to produce iron from its ore with pure oxygen gas as the only direct emission.

The feasibility of MOE as a carbon-neutral process hinges on the identification of an inert anode material. Therefore, the scope of this study was to determine the criteria of an inert anode for MOE, identify candidate materials, and evaluate the performance of these materials. Previous studies of MOE at MIT found iridium, a platinum group metal, to be an excellent candidate for an inert anode. The high cost of iridium makes it an unlikely candidate for a commercial iron production process. However, iridium provides a likely candidate for lunar production of oxygen, or high-purity iron production. Furthermore, the use of iridium on the laboratory-scale provides a widely available inert anode material to facilitate the study of other areas of MOE. Therefore, unique anode morphologies were evaluated as a means to reduce the economical strain of using an iridium anode.

In addition to iridium, a wide array of readily available, high-temperature electrode materials were tested. Due to the highly corrosive environment of MOE, none of the readily available materials tested are compatible with the process. It is believed that the most likely candidate for an inert anode lies in an engineered material, composed of a refractory substrate and an oxide passivation layer. Therefore, the criteria for such a material were determined and likely candidates are discussed.

Thesis Supervisor: Donald R. Sadoway
Title: John F. Elliot Professor of Materials Chemistry

BIOGRAPHICAL NOTE

James D. Paramore was born and raised in Salt Lake City, Utah. During his undergraduate education at the University of Utah, James had the opportunity to participate in research of various metallurgical fields including electrowinning of copper, room-temperature electrolysis of titanium, and production of bulk-nanocrystalline refractory materials. His most extensive undergraduate research opportunity was enjoyed during his last three years as an undergraduate, in which he helped develop a new powder metallurgical process to produce bulk nanocrystalline refractory materials under the supervision of Professor Z. Zak Fang. Professor Fang is a truly extraordinary mentor, affording James trust and responsibility that accelerated his scientific maturation. James was Professor Fang's primary researcher on a grant to research the production of nanocrystalline tungsten penetrators for the Army Research Laboratory (ARL). Professor Fang allowed James to attend and present at several technical conferences, as well as prepare and present quarterly updates to ARL. In addition to his research responsibilities, James also served as a teaching assistant for *Introduction to Physical Metallurgy* at the University of Utah.

James received several scholarships and awards as an undergraduate including the 2008 Materials Processing & Manufacturing Division Scholarship from TMS, 2007 Lucille & Charles A. Wert Scholarship from ASM, 2007 Kennecott Scholarship, 2007 Rio Tinto Scholarship, 2006 George A. Roberts Scholarship from ASM, and the 2006 Oblad Energy Scholarship, among others. James graduated *magna cum laude* from the Department of Metallurgical Engineering at the University of Utah. Upon arrival at MIT in Fall 2008, James was first introduced to Professor Donald Sadoway as a teaching assistant for *3.091: Introduction to Solid-State Chemistry*. In Spring 2009, James continued as the 3.091 teaching assistant under Professor David Paul before joining Professor Sadoway's research group on the molten oxide electrolysis project in Summer 2009. Professor Sadoway has been an extraordinary mentor and inspiration to James, and has been a huge influence in James' life ever since.

In addition to his academic endeavors, James is a passionate musician. In fact, James started off his undergraduate education as a music major in piano, before deciding that music better suited him as a hobby, rather than a career. However, James worked as a professional club DJ in Utah during his undergraduate education, and performed at various music festivals as a keyboardist.

PREVIOUS PUBLICATIONS

J. Paramore, Z. Fang, H. Zhang, X. Wang, D. Siddle & K. Cho, "Production of Nanocrystalline Tungsten Using Ultra-High-Pressure Rapid Hot Consolidation (UPRC)." *Advances in Powder Metallurgy and Particulate Materials*, **2** (2007)

A. Shchetkovskiy, T. McKechnie, D. R. Sadoway, J. Paramore & O. Melendez, "Development and Testing of High Surface Area Iridium Anodes for Molten Oxide Electrolysis." *Proceedings of Earth and Space 2010*, **4** 1039 (2010)

PENDING PUBLICATIONS

H. Kim, J. Paramore, A. Allanore, D.R. Sadoway, "Stability of Iridium Anode in Molten Oxide Electrolysis for Ironmaking: Influence of Slag Basicity." *ECS Transactions*, **29** (2010)

ACKNOWLEDGEMENTS

I thank the American Iron and Steel Institute (AISI) and the National Aeronautics and Space Administration (NASA) for their financial sponsorship.

I would like to thank each of the following individuals and groups who have aided in the completion of this thesis:

Professor Sadoway, for seeing potential in me, always fighting on my side, and for all his words of inspiration which helped me through some doubtful times. He is a true lifelong friend and mentor.

Dr. Hojong Kim, for all his kind help and long hours spent with me in the lab, and for his constant readiness to sit down with me and talk about the often confusing results from our experiments.

Dr. Antoine Allanore, for all of his hard work on the MOE project and his seemingly endless ambition to tackle the problems we faced, as well as his constant honesty about my results.

Mr. Mike Tarkanian, for spending hours upon hours training me on all the machining equipment in our department, as well as coming at a moment's notice to help me fix a machine that broke.

Mr. Guenter Arndt, for always being ready, willing, and happy to help pursue whatever tedious work I would bring him.

Ms. Hilary Sheldon, for always having the answer to administrative questions and saving my rear-end on more than one occasion.

Everybody in the Sadoway research group, whose camaraderie and kindness made it a pleasure to come to work everyday, and for always being willing to lend a hand whenever possible.

Ms. Anna Henry, for moving with me 2500 miles away from her friends and family, and for helping me through the stress and frustration that comes with graduate studies.

I dedicate this thesis to my parents, Ray and Nancy Paramore, who I know have been on an emotional roller-coaster ride throughout my upbringing. I was a hard pill to swallow at times, but they always put immeasurable trust and confidence in my abilities, and supported me all along the way. I know that, regardless of circumstance, they will make the greatest of sacrifice if there is even the slightest chance that it will positively affect my wellbeing, and for that I am truly grateful.

My time at MIT has been a mixture of tribulations and celebrations. While I leave this extraordinary institution with a vast knowledge of science and engineering, I have also been taught valuable lessons on humanity and social responsibility; things which are often lost in the abstractions of science. I will dedicate my life to continuing these awesome traditions and strive to be a worthy progeny of my mentors.

Table of Contents

Chapter 1: Introduction.....	7
1.1 Motivation.....	7
1.1.1 Iron Production.....	7
1.1.2 Lunar Production of Oxygen.....	8
1.2 Fundamental MOE Considerations.....	9
1.2.1 Basic Cell Design.....	10
1.2.2 Inert Anode Criteria.....	11
1.2.2.1 Platinum Group Metals.....	12
1.2.2.2 Oxide Passivated Metallic Anodes.....	13
1.2.2.3 Cermet Anodes.....	15
1.2.3 Electrolyte Criteria.....	15
1.2.3.1 Optical Basicity	16
1.3 Summary.....	18
Chapter 2: Experimental Design.....	21
2.1 Cell Design.....	21
2.1.1 Furnace Assembly.....	21
2.1.1.1 Design Improvements.....	23
2.1.2 Materials Candidates.....	25
2.1.2.1 Anode.....	26
2.1.2.1.1 Iridium Anodes.....	26
2.1.2.1.1.1 Unique Morphologies.....	27
2.1.2.1.2 Other Anode Materials.....	28
2.1.2.2 Cathode.....	29
2.1.2.3 Crucibles.....	30
2.1.2.3.1 Effect of Electrolyte Basicity on Crucible Selection.....	30
2.1.2.3.2 Novel Crucible Design.....	31
2.2 Electrolyte Selection.....	33
Chapter 3: Experimental Results.....	35
3.1 Iridium.....	35
3.1.1 Electrodeposited Iridium Anodes.....	35
3.1.2 Effect of Electrolyte Basicity on Iridium Anodes.....	38
3.1.3 Results from Novel Crucible Design.....	42
3.2 Other Candidate Anode Materials.....	44
Chapter 4: Implications of Experimental Results and Future Considerations.....	47
4.1 Proposed Corrosion Mechanism for Iridium Anodes.....	47
4.1.1 Suggested Experimentation to Quantify Corrosion Rate of Iridium.....	51
4.2 Anodes with Different Corrosion Mechanisms.....	53
4.3 Cold-Wall Cells for the Next Scale.....	57
Chapter 5: Concluding Remarks.....	59
References.....	61

Chapter 1: Introduction

1.1 Motivation

Molten oxide electrolysis (MOE) uses electric current to reduce the metallic cation of an oxide to its pure form, while oxidizing the corresponding oxide anions into oxygen gas. Therefore, the study of this process has been motivated by the acquisition and use of these two products. The production of iron metal from an iron oxide containing electrolyte has been studied as a carbon-neutral approach to replace current pyrometallurgical processes that result in copious amounts of greenhouse gas emissions. Furthermore, the production of oxygen gas at the anode has been studied as a means to produce oxygen on the surface of the moon. While stemming from the same fundamental reaction, these two goals present unique challenges and feasibility criteria.

1.1.1 Iron Production

Iron is by far the most widely used metal. The majority of iron produced from ore is still achieved using antiquated blast furnace technology; which produces nearly 2 metric tons of carbon dioxide per metric ton of crude iron produced [1]. Furthermore, the vast majority of steel produced today is accomplished with a limited number of processes and nearly identical raw materials [1]. In terms of cost and efficiency, there has been little need for improvement of these highly efficient technologies over the centuries. However, despite the economical attractiveness, the environmental impact is substantial. In addition to carbon emissions from blast furnaces, the iron and steel industry contributes to greenhouse gas (GHG) emissions in several ways. Sources of GHG emissions from the iron and steel industry include: blast furnace emissions, coke production emissions, use of carbonate flux during calcination, and emissions from carbon electrodes in electric arc furnaces [2].

The iron and steel industry is currently responsible for 3-4% of the total worldwide greenhouse gas emissions [3]. In 2006, iron and steel mills produced 126 million metric tons of carbon dioxide [4]. While there have been myriad improvements to the intricacies of modern steelmaking since its introduction during the industrial revolution, nearly all crude iron

production today is accomplished using the same fundamental carbothermic processes. As a primary contributor of global GHG emissions from the industrial sector, the iron and steel industry has been under constant scrutiny from various national and international environmental associations such as the U.S. EPA, the EIA, and IEA [1;2;4;5]. There have been great strides made by iron and steel mills to reduce GHG emissions through innovations made on legacy technologies. However, in order to realize a truly efficient, carbon-neutral technology, a radically different technology using fundamentally different extractive metallurgy is required.

Upon the use of an inert anode, molten oxide electrolysis (MOE) is theoretically capable of producing tonnage metal with oxygen gas as the only direct emission. Compared to other electrochemical extractive techniques, molten oxide electrolysis has several advantages including:

- Minimal pretreatment of the oxide ore feedstock is required
- The molten oxide electrolyte has low vapor pressure above 1538°C
- Iron produced at the cathode is molten and ready for continuous casting

Some of the primary criteria for developing a commercial MOE process to produce iron and steel are economical considerations. With regards to industrial applications, this becomes a major factor. However, because MOE directly reduces iron oxide to iron metal, if carbon-free iron oxide feedstock is used, the product of MOE is high-purity iron metal. High-purity iron is currently an extremely expensive commodity in relation to steel, due to the elaborate processing required to remove the highly soluble carbon from carbothermically reduced crude iron [6]. Therefore, if MOE fails to develop into an economically feasible process for steelmaking, it could still be a viable one-pot alternative for the niche market of high-purity iron.

1.1.2 Lunar Production of Oxygen

The cost of transporting materials to the moon is approximately 100,000 USD per kilogram [7]. Nearly all of this cost is associated with the energy requirements to escape Earth's gravity.

Therefore, the feasibility of sending manned missions beyond the moon relies on the ability to launch missions from the Moon's considerably weaker gravitational hold. Considering that a large portion of the payload for any mission will be oxygen as an essential raw material for rocket fuel, as well as human life support, the ability to produce oxygen on the surface of the moon is a necessary prerequisite for future deep space exploration. The surface of the Moon is covered with a layer of regolith, which is a loose, rocky mixture of metal oxides (Table 1.1). Therefore, using lunar regolith as the feedstock for a MOE cell, future lunar missions would be equipped with the ability to not only produce oxygen, but also produce iron and silicon as raw materials for a lunar base.

Table 1.1: Approximate composition of lunar regolith.

<u>Chemical</u>	<u>Wt%</u>
SiO ₂	47.3
Al ₂ O ₃	17.8
CaO	11.5
FeO	10.5
Fe ₂ O ₃	0
MgO	9.2
Na ₂ O	2.7
TiO ₂	1.6
K ₂ O	0.8
P ₂ O ₅	0.7
MnO	0.1

1.2 Fundamental MOE Considerations

Previous work done at MIT has successfully addressed the fundamental electrochemistry of MOE [7;8]. Therefore, this study focuses primarily on the feasibility and engineering challenges associated with scale-up of the MOE process. The pièce de résistance is, without doubt, the attainment of an inert anode material. However, other materials challenges must be addressed for the progressive scale-up steps on the road to commercial MOE. Optical basicity of the electrolyte and current density are the metrics used in this study to determine feasibility of electrode and crucible materials for the process' scale-up.

1.2.1 Basic Cell Design

The Hall-Héroult cell used in the aluminum industry may be studied as a basic representation for the MOE process (Figure 1.1). However, the MOE process presents several unique materials challenges:

- Extremely high operating temperatures ($>1538^{\circ}\text{C}$) expedite corrosion reactions
- Strong oxidizing environment due to evolution of pure oxygen and anodic potential
- Metal solubilizing liquid metal product
- Ceramic solubilizing molten oxide electrolyte

Therefore, in order to overcome these challenges, an industrially feasible cell must have the following characteristics.

- Inert anode capable of resisting the highly corrosive environment
- Thermal gradient to allow molten electrolyte to freeze at the extremities of the cell, therefore, protecting the refractories used to contain the bath

Similar to a Hall-Héroult cell, an MOE cell will use joule heating to maintain operating temperatures ($>1538^{\circ}\text{C}$ for an MOE cell), circumventing the need for fossil fuel heating.

Previous studies have demonstrated the fundamental feasibility of the process by showing successful electrolysis of molten oxide electrolytes [7;8]. Current efficiencies, when measured with respect to oxygen generation, varied between 30 – 60% during electrolysis in iron-containing electrolytes, and between 60 - 100% in iron-free electrolytes [7]. The discrepancy in current efficiency measurements with respect to the presence of iron is believed to be the result of two phenomena: aliovalent cycling between ferrous and ferric ions, and electrolytic short-circuiting caused by electronic conductivity of iron oxides [7].

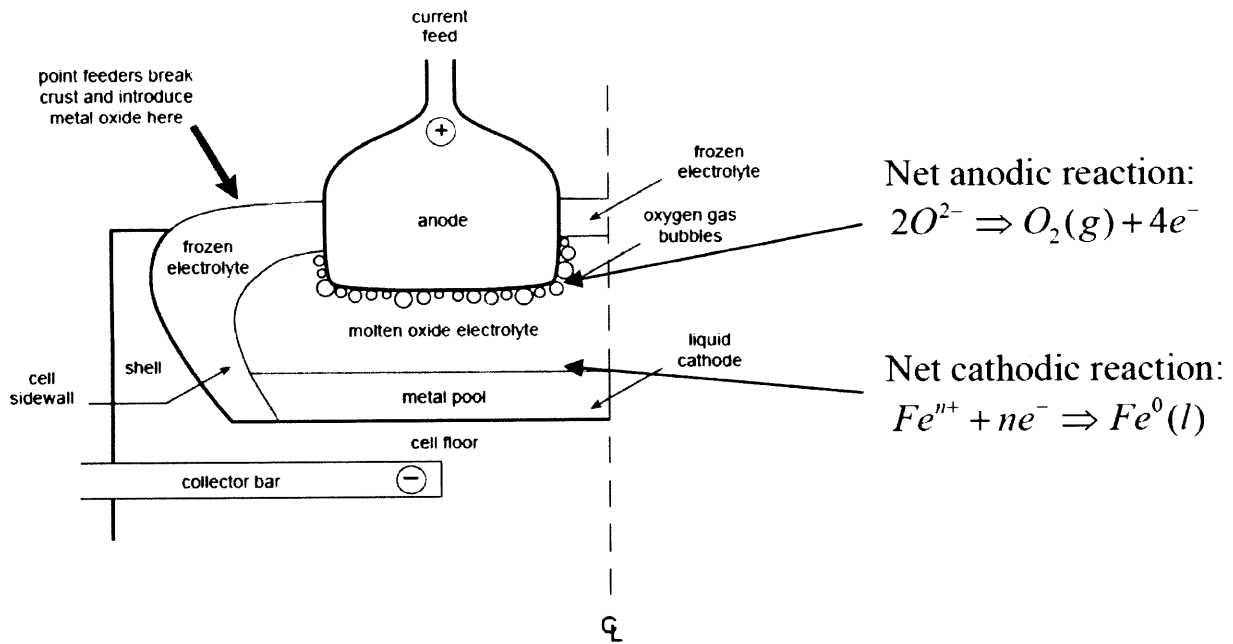


Figure 1.1: Theoretical schematic of an industrial MOE cell [8].

1.2.2 Inert Anode Criteria

The ability for MOE to be a truly carbon-neutral method for producing iron relies on the identification of a suitable inert anode material. The aluminum electrowinning industry uses carbon anodes in the Hall-Héroult cell, which participate in the anodic reaction and evolve carbon dioxide gas. Therefore, the acquisition of an inert anode will have the greatest implication as to whether or not MOE is a viable, carbon-neutral process for iron production. The aluminum industry has put great effort into the search for an inert anode. As the Hall-Héroult cell is the nearest industrial equivalent to MOE, the MOE criteria for an inert anode have been adapted from the criteria used by the aluminum electrowinning industry:

1. Less 10 mm/year linear loss of anode material [9]
2. Physically stable above 1538°C [10]
3. Resistant to attack by molten oxide electrolyte [10]
4. Resistant to attack by pure oxygen at extremely high temperatures [10]

5. Resistant to anodic (oxidizing) polarization [10]
6. Electronically conductive [10]
7. Resistant to thermal shock from lowering into molten oxide bath [10]
8. Mechanically robust [10]
9. Simple to deploy during startup and in case of power interruptions [10]
10. Economically feasible and widely available to meet the demands of the iron and steel industry

With the above criteria in mind, the possible materials candidates are discussed below.

1.2.2.1 Platinum Group Metals

The platinum group metals (PGM) are widely used in the glass industry due to their excellent corrosion resistance in molten oxide glasses [11]. All of the platinum group metals, with the exception of ruthenium, are very expensive and are, therefore, ruled out as a pure anode material for steelmaking by criterion number 10 listed above. However, PGMs may be viable candidates for high-purity iron making (refer to last paragraph of section 1.1.1) and lunar production of oxygen; even in these applications it is likely the PGM will be in the form of a thin coating or as a small-concentration constituent in an alloy. Despite their unlikely transition to an industrial-scale option, PGMs have shown to be promising inert anode candidates, and provide long-lasting, readily available anode materials for laboratory-scale studies. Therefore, while use of PGMs for commercial steel production is prohibited by cost, these materials are very valuable to use as anodes during studies of other areas of the MOE process. Table 1.2 provides a list of the six PGMs and their advantages and disadvantages with respect to MOE.

Ruthenium, palladium, and osmium each have at least one property that is unavoidably incompatible with operating conditions of an MOE cell. Therefore, these metals were ruled out and investigation was never pursued. Previous work at MIT with the three remaining PGMs found iridium to be the most likely candidate as an inert anode material [8].

Table 1.2: Advantages of disadvantages of platinum group metals in regard to MOE.

Metal	Advantages	Disadvantages
Ruthenium	Inexpensive PGM ~\$6/g	Volatile at high temperatures in O ₂ [12]
Rhodium	N/A	Extremely high cost ~\$71/g
Palladium	N/A	Melting temperature too low Cost ~\$16/g
Osmium	N/A	Volatile at high temperatures in O ₂ [12] Cost ~\$12/g
Iridium	Most noble metal Melting temperature = 2446°C Resistant to molten oxides	High hardness → difficult to machine Cost ~\$23/g
Platinum	Very noble metal Resistant to molten oxides	Cost ~\$50/g Melting temperature = 1768°C

1.2.2.2 Oxide Passivated Metallic Anodes

An oxide passivated anode will likely be the best inert anode material if a suitable alloy can be found. The idea behind protective oxide layers was first described by Pilling and Bedworth in 1923 [13], and is utilized ubiquitously in corrosion resistance today. This phenomenon is when a metallic substrate, normally vulnerable to corrosion, is protected by an oxide layer which separates the metal from the environment. The oxide layer can either be grown on the substrate using an oxidizing environment or anodic potential, or physically placed on the substrate using sputtering, chemical vapor deposition or colloidal deposition [14]. In the case of MOE, it is likely that a system of two main components will be engineered: a refractory metal substrate alloyed with a reactive solute metal. If the solute metal is sufficiently reactive, it should preferentially oxidize to form the protective oxide layer.

The Pilling-Bedworth ratio (R_{PB}) is a first approximation used to determine if an oxide will protect a metallic substrate. The ratio is calculated by dividing the molar volume of the oxide by the molar volume of the substrate metal [13]. If the ratio is much larger than 1, the oxide will tend to buckle and chip, causing the underlying metal to be exposed [13]. If the ratio is much smaller than 1, the oxide will not sufficiently cover the substrate, thereby allowing it to corrode [13]. There are many exceptions to this simple rule. However, this is the underlying theory of an oxide passivated inert anode. In order for an oxide passivated anode to work, there are

several criteria for the oxide layer, in addition to $R_{PB} \approx 1$, that must be met:

1. Electronically conductive to allow electrons to pass into the anode during the oxide ion oxidation reaction
2. Not conductive to oxide ions, as this would allow unmitigated growth of the oxide layer at the metal/oxide interface
3. Not conductive to either the solvent or solute cations, as this would allow consumption of the substrate or unmitigated growth of the oxide layer at the oxide/electrolyte interface, respectively
4. Not soluble in the multi-component molten oxide electrolyte

The oxide passivated anode has several key advantages over other possible candidates. The metallic substrate provides the bulk mechanical properties of the anodes, giving it the desired thermal shock resistance, toughness, and ease of machinability characteristic of metals. The metallic substrate will also have excellent electronic conduction. However, while the oxide layer protects the underlying substrate from corrosion, it also passivates the electric current. Therefore, in order to allow the necessary faradaic processes to occur at the surface of the anode, the oxide layer will have to support some form of electronic conduction.

Most oxides have large band gaps, resulting in poor electronic conduction. However, at MOE operating temperatures ($>1538^{\circ}\text{C}$), some oxides exhibit semiconduction due to the high degree of thermal excitation. Therefore, use of one of these oxides should facilitate electronic transfer across the oxide passivation layer.

If an oxide is selected that exhibits no form of electronic conduction, the oxide layer will need to be thin enough to allow for electron tunneling. Generally, electron transfer rate, k^0 , decreases exponentially with the distance of tunneling, x , by the following equation:

$$k^0(x) = k^0(x=0) \exp(-\beta x) \quad (1)$$

where β is independent of potential and on the order of 1 \AA^{-1} [14]. Therefore, in order to allow

for effective tunneling, the oxide must be extremely thin ($x < 1.5\text{nm}$), and even thinner in the case of highly resistive oxides, such as those of aluminum and tantalum [14].

1.2.2.3 Cermet Anodes

A cermet is a metal/ceramic composite. Cermets, like any composite, are engineered to combine positive attributes of the two phases. With respect to inert anodes, this would be the corrosion resistance of the ceramic and the electronic conductivity and toughness of the metal [10]. Cermet anodes consisting of a ceramic matrix with metallic dispersions have been researched by the aluminum industry with varying results [10]. For example, success has been enjoyed in laboratory-scale aluminum electrowinning cells with cermet anodes, such as copper/nickel impregnated nickel-ferrite [15]. However, despite promising performance at the small scale, the poor thermal shock resistance of the ceramic matrix caused catastrophic failure of the anodes upon lowering into the cryolite bath during pilot-scale tests [16].

It is unlikely that a cermet with a ceramic matrix will ever have the necessary thermal shock resistance to serve as an anode in an MOE cell. However, if a metal was found with corrosion resistance that was on the borderline of the inertness criterion, then a cermet could be engineered with that metal as the matrix with a ceramic dispersion. The ceramic dispersion would give the metal the small boost in corrosion resistance it needed to qualify as an inert anode. The theory behind such a cermet is that the ceramic dispersion would lower the active surface area of the metal exposed to the electrolyte. Therefore, the dispersion should reduce the corrosion kinetics of the metal, but the metallic matrix should impart the attractive mechanical properties of the metal to the cermet.

1.2.3 Electrolyte Criteria

The chemistry of the electrolyte greatly influences process parameters and materials compatibility issues. For the lunar project, the nominal electrolyte chemistry is set by the composition of the mandatory feed material, lunar regolith (approximate average composition of

lunar regolith is listed in Table 1.1). However, for the iron project, the electrolyte may be engineered. The following criteria must be kept in mind while determining the appropriate electrolyte chemistry:

1. Melting temperature below 1538°C to limit heating power needs
2. Low vapor pressure of above 1538°C
3. Minimum viscosity at operating temperatures to facilitate fast oxygen bubble escape
4. Minimum possible electronic conductivity (to maximize current efficiency)
5. Maximum possible ionic conductivity
6. Minimum corrosiveness towards electrodes and refractories¹

The complexity of multi-component oxide systems makes quantifying the physical properties of these systems extremely difficult. Therefore, considerations of criteria 1-4 were explored by painstaking study of multi-component oxide system phase diagrams, as well as literature on well known oxide slags used in the steel and glass industry [17;18]. However, the ionic conductivity and solubilizing strength of molten oxides both tend to vary as a function of the slag's basicity. Therefore, a more quantitative approach was applied to criteria 5 and 6 by using the electrolyte's basicity as a metric.

1.2.3.1 Optical Basicity

There are important implications for the properties of a molten oxide that may be drawn from the slag's basicity (i.e. ionic conductivity, solubilizing strength, and redox equilibria of aliovalent species within the melt). Similar to aqueous systems, molten oxide systems tend to exhibit either a more acidic or more basic nature. The Lux-Flood formalism is used to define the acidic/basic nature of an oxide by evaluating the oxide's propensity to accept or donate, respectively, an oxide ion during interaction with another oxide [19]. As one can see, this is a direct extension of Lewis acid/base formalism used to define acids and bases as electron pair acceptors or donors, respectively. In the case of oxide systems, the oxide ion (with a charge of -2) may be thought of

¹ This consideration is only important at the laboratory-scale, as a production cell will have a frozen electrolyte to protect the refractories.

as an electron pair. While the Lux-Flood formalism provides a useful tool for envisioning the reaction mechanism in oxide systems, it lacks the ability to easily quantify these acid/base qualities for data analysis. Therefore, in order to quantify the acidic or basic nature of an oxide, one may use the optical basicity scale.

Optical basicity is a quantitative scale based on the bonding characteristics of a Lewis acid/base pair (in this case, Lux-Flood acid/base pair). The term “optical basicity” stems from the use of optical spectroscopy as a tool to experimentally measure optical basicity; this process is described in detail for several metal oxides by Duffy [20]. The optical spectroscopy method measures the frequency shift of adsorption bands of tracer ions such as Tl^+ , Pb^{2+} , or Bi^{3+} , from free ions to ions contained within the slag, and defines optical basicity as [17]:

$$\Lambda = \frac{\text{Electron donor strength of slag}}{\text{Electron donor strength of CaO}} = \frac{\nu_{free} - \nu_{slag}}{\nu_{free} - \nu_{CaO}} \quad (2)$$

The basicity of an elemental oxide (i.e. its propensity to donate its oxide ion) increases as the negative charge concentrated on the oxide ion increases [20]. Therefore, properties of the cations that dictate the electron distribution, such as oxidation state and electronegativity, may be used for theoretical calculations. Theoretical optical basicity, Λ_{th} , can be accurately calculated for many oxides from Pauling electronegativities [17]. As can be observed in equation (2), calcia is used as the standard with an optical basicity of 1.0.

Optical basicity is especially useful for multi-component oxide systems, as the optical basicity of any system may be calculated as the weighted average of the optical basicities of its constituents by the following equation:

$$\Lambda_{slag} = \frac{\sum_i n_i x_i \Lambda_{th,i}}{\sum_i n_i x_i} \quad (3)$$

where x is the stoichiometric coefficient and n is the number of oxygen atoms in the oxide (i.e. for Al_2O_3 $n=3$) [17]. Unless otherwise noted, optical basicity values reported in this study have

been calculated using equation (3) and the data in Table 1.3.

Table 1.3: Selected optical basicities. Adapted from [17].

Oxide	Λ from U.V. shift	Λ from Pauling E.N.	Recommended Λ
Li ₂ O	1.00	1.0	1.0
Na ₂ O	1.15	1.15	1.15
K ₂ O	N/A	1.40	1.4
MgO	0.78	0.78	0.78
CaO	1.0	1.0	1.0
Al ₂ O ₃	0.605	0.60	0.605
SiO ₂	0.48	0.47	0.48
TiO ₂	N/A	0.61	N/A
P ₂ O ₅	0.40	0.40	0.40
MnO	N/A	0.59	1.0
FeO	N/A	0.51	1.0
Cr ₂ O ₃	N/A	N/A	0.8
Fe ₂ O ₃	N/A	0.48	0.8

1.3 Summary

In this chapter, the motivation behind investigating MOE as a replacement for antiquated iron and steel production technologies was discussed. Upon identification of a suitable inert anode, MOE will have the ability to produce tonnage-scale iron with oxygen gas as the only direct emission. In addition to this very substantial motivation, the process also has esoteric applications. The composition of lunar regolith makes MOE an attractive choice for lunar production of oxygen, iron, and silicon. Furthermore, because the process does not use any form of carbothermic reduction, the iron product produced by MOE is free of the highly soluble carbon interstitials. Therefore, MOE could be a more cost effective method for producing high-purity iron metal. This chapter also briefly introduced some of the fundamental science that will be used throughout the discussions in the following chapters.

Chapter 2 details the design of the experiments used to investigate possible inert anodes for MOE. This chapter will also discuss the implications the corrosiveness of the electrolyte has on other materials issues associated with MOE experiments.

Chapter 3 presents the experimental results obtained during this study.

Chapter 4 dissects the results from Chapter 3 for implications on the feasibility of MOE and development of an inert anode. This chapter also contains a proposed experimental plan to further understand the reaction mechanisms of iridium anodes, as well as recommendations for likely inert anodes besides iridium.

Chapter 5 reiterates the environmental significance of an industrial-scale MOE process for iron production and summarizes key points discussed throughout the manuscript.

Chapter 2: Experimental Design

The primary goal of this study was to continue previous MOE research conducted at MIT and evaluate the performance of candidate anode materials during long experiments (>4 hours) with increased surface area (50~100 cm²), as well as to propose and test hypothetical mechanisms for anode failure.

2.1 Cell Design

One of the primary engineering issues that must be faced on the road to developing a commercially feasible MOE process is the design of a self-heated, cold-walled cell. However, at this stage it was considered a superfluous enterprise, because the cell dimensions necessary to achieve sufficient joule heating would be extremely expensive to construct for an unproven process. Therefore, external heating was used to reach and maintain operating temperatures in excess of 1538°C.

2.1.1 Furnace Assembly

Table 2.1: Vertical tube furnace properties.

Furnace Manufacturer	Tube Dimensions		Maximum Temperature (°C)	Heating Element Material
	ID x OD x Height (in)	McDanel 99.8% Al ₂ O ₃		
Carbolite	4.125 x 4.5 x 32		1800	LaCrO4
Mellen	4.125 x 4.5 x 30		1800	MoSi ₂
Mellen	8.0 x 8.5 x 32		1800	MoSi ₂

All the experiments in this study were conducted in one of three resistance-heated, vertical tube furnaces (Table 2.1). The 8.0" ID Mellen furnace was acquired for further scale-up experiments. However, the extremely expensive consumable refractory materials necessary to operate this

furnace made experimentation cost prohibitive. Therefore, the vast majority of experiments detailed in this thesis were conducted in one of the two 4.125” furnaces.

Both heating element materials have limitations with respect to ramp rates. Therefore, all experiments were conducted with ramp rates no greater than 100°C/hr to ensure maximum life of heating elements. As per the design of the temperature controllers, process value (PV) was determined using type B thermocouples located inside the hot zone of the furnace, but outside of the furnace tube. This arrangement was necessary in order to maintain a controlled atmosphere during experimentation. Obviously, this setup meant that the process value on the temperature controller was greater than the actual operating temperature of the electrolysis cell. In order to overcome this challenge, temperature profiles were measured on all furnaces using a 36” type B thermocouple, which was fed into furnace through a Swagelok Ultra-Torr™ fitting on the furnace cap. The smaller Mellen furnace had a temperature differential of ~100°C, while the Carbolite furnace had a temperature differential of ~50°C, due to superior insulation of radiant heat. The temperature differential on the 8” furnace varied considerably, depending on the crucible assembly of the experiment. Therefore, an internal thermocouple was always used with the 8” furnace for real-time measurements of the electrolysis cell.

As mentioned above, the goal of this study was to determine the performance of the anode during scaled-up electrolysis experiments. Therefore, experiments were conducted using one working electrode (anode) and one counter electrode (cathode), with no reference electrode.

The greatest factor limiting the length of the experiments was crucible failure. The molten oxide electrolyte has great solubilizing strength of traditional ceramic crucible materials. Therefore, experiments were always conducted using a two crucible design. The electrolyte was contained within a ceramic primary crucible. The primary crucible was then placed within a secondary crucible, which was partially filled with absorbent alumina beads. The furnace tube was then filled partially with additional alumina beads. The goal of this design was to prevent damage the prohibitively expensive furnace tubes or, even worse, the furnace itself. However, as research began on the different electrolyte compositions, it became apparent that crucible redundancy was only effective with certain electrolyte chemistries. Materials engineering challenges with respect

to refractories will be discussed in detail in section 2.1.2.3.1.

2.1.1.1 Design Improvements

As mentioned above, one of the key challenges associated with MOE is the expedited corrosion reactions caused by the extremely high temperatures and presence of oxygen. Additionally, an important tool for analyzing current efficiency was measuring oxygen concentration of furnace exhaust. Therefore, it is extremely important that the experimental environment remain uncontaminated by the surrounding atmosphere. The cell cap design that was used in previous MOE studies at MIT [8] was determined to be insufficient for the scale-up of the investigation. Therefore, a new cell cap capable of consistently providing a perfect seal was invented.

Previous MOE studies at MIT used a cell cap that sealed to the furnace tube by using a steel collar that fit around the furnace tube, with an O-ring between the outer furnace tube wall and the inner wall of the steel collar [8]. An airtight seal was achieved when the clearance between the outer furnace tube wall and inner steel collar wall was small enough that forcing the collar and O-ring over the furnace tube caused the O-ring to compress and gasket to the tube and collar. However, it was found that if the clearance was too small, it was nearly impossible to get the collar onto the furnace tube without breaking the fragile ceramic tube. Furthermore, if the clearance was too large, the O-ring would not form a gasket. Even if an airtight seal was achieved, the seal would fail if internal pressure of the furnace tube exceeded 1 atm; which was a common occurrence during heating of the furnace. After an extensive search of tube furnace accessories vendors came up empty, the invention of a more robust sealing system was undertaken.

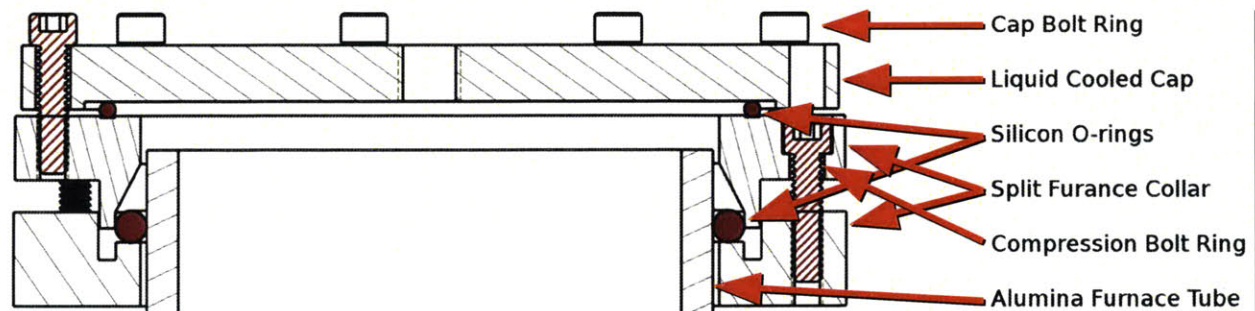


Figure 2.1: Cross-section of new furnace cap/collar design.

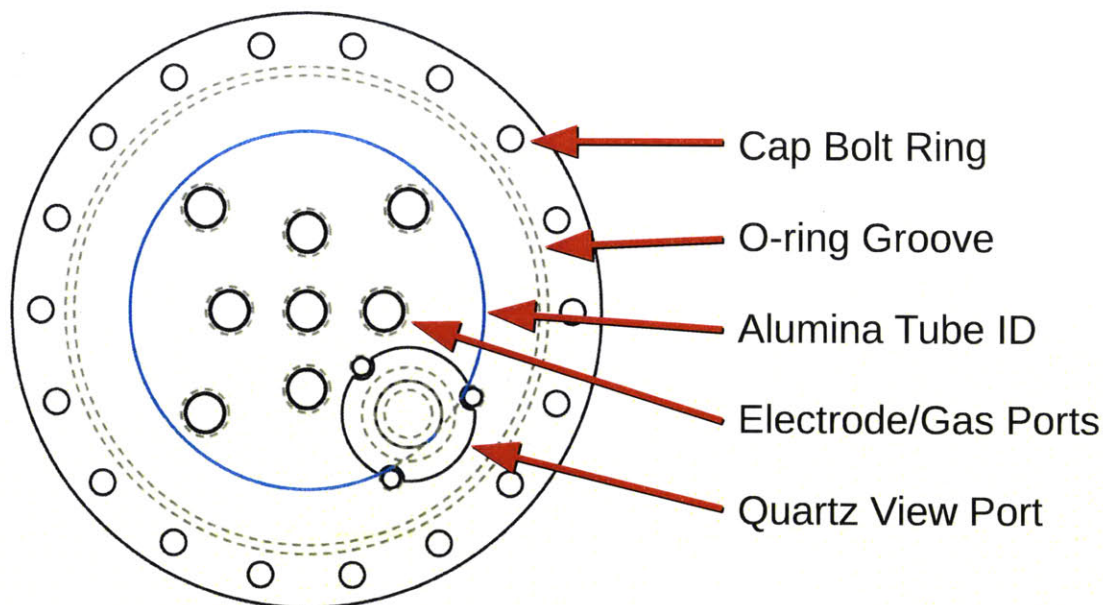


Figure 2.2: Top view of liquid cooled furnace cap with view port.

The author recognized the need for a mechanical compression fitting. This type of fitting would allow the furnace collar to easily slide over the tube, and be subsequently tightened to form a robust gasket. The slip casting method used by the furnace tube vendor (McDanel Advanced Ceramics) results in large radial tolerances of the furnace tubes (OD 4.50" \pm 0.180"). Therefore, the mechanical compression fitting had to have a change in internal diameter, upon tightening, that spanned the 0.180" furnace tube tolerance plus the change in O-ring diameter to achieve the nominal vacuum-rated contact pressure of 13 kg/cm² [21]. The new compression fitting works by using a bolt ring to join a split collar with a sliding, beveled O-ring groove that compresses a -425 silicone O-ring (McMaster-Carr Part:9396K363) to the furnace tube (Figure 2.1). The resulting design has been tested, with a new silicone O-ring, to 20 psi (138 kPa) positive internal pressure differential (equal to 1.4 kN of longitudinal force on the furnace cap), with the furnace PV at 1600°C, without any detectable leaks.

As mentioned above, an inert atmosphere was crucial for MOE experiments. The MOE cell assembly used in previous studies at MIT achieved an inert atmosphere by purging the furnace with helium for extended periods of time (>12 hours). It is well known that purging with helium can be notoriously difficult, due to its low density. The MOE experiments are particularly difficult to purge due to the porous material used (powder preparation of electrolyte, and use of

alumina beads), and the necessity for the gas inlet to be above the electrolysis bath. Because of this, extremely large amounts of inert gases were used to purge the system. Even then, anomalous spikes in oxygen would be detected during experiments. These oxygen spikes were believed to be caused by degassing of trapped gas during the melting of the electrolyte, or the escape of gas pockets in the alumina beads due to convection upon heating. Previously, the use of a vacuum-purge procedure was avoided due to fear of atmospheric pressure fracturing the fragile furnace tube when under vacuum. However, it was quickly realized that alumina ceramic is only fragile with respect to tensile stresses, and should be able to easily withstand an evenly distributed compressive force caused by a negative pressure differential inside the furnace tube. Therefore, a vacuum-purge system was designed and installed, instantly making the use of large volumes of inert gas obsolete for purging, as well as eliminating the occurrence of anomalous oxygen spikes.

The final innovation made to the MOE assembly was the design and installation of a view port. As mentioned above, the length of the experiments were determined by the maximum service life of the ceramic crucibles. Despite the redundancy of the crucibles, the molten electrolyte is capable of breaching both crucibles and damaging the expensive furnace tubes and, in some cases, capable of eating through the furnace tubes and damaging the furnace itself. Previously, crucible failure was determined by the loss of electrolytic current. When the electrolyte would breach the primary crucible, the bath level would drop below the height of the anode, causing the electrolysis circuit to open and the current to stop. At this point, the experiment would be immediately stopped. However, due to the slow ramp-down rate ($<100^{\circ}\text{C/hr}$), it was possible that the electrolyte would continue to breach the secondary containment crucible before the electrolyte would solidify. Therefore, the need for a view port was mandated; not only to protect against crucible failure, but also as a means to observe oxygen evolution during electrolysis (Figure 2.2).

2.1.2 Materials Candidates

Fundamentally, the MOE process may be categorized as a novel extractive metallurgical

technique. However, the practical engineering challenges associated with constructing a working MOE cell call upon the sagacity of the researcher with respect to corrosion engineering and materials compatibility. Not only does the cell require exceptional materials properties as a whole, but the individual components must be considered with regard to their unique corrosive environments. Therefore, the cell must be broken down into its three major parts (anode, cathode, and crucible/refractories) to determine appropriate materials.

2.1.2.1 Anode

Despite nearly a century of industrial maturation, the aluminum industry has yet to find a suitable inert anode that can withstand the highly corrosive environment and meet the electrochemical and mechanical demands of the Hall-Héroult cell [9;10]. With even higher operating temperatures and faster corrosion kinetics, the search for an inert anode for the MOE cell is a materials engineering challenge in a class of its own. Possible materials classes under investigation are discussed in detail in Chapter 1. This study focused primarily on iridium anodes. However, various materials have also been investigated as possible anode candidates.

2.1.2.1.1 Iridium Anodes

Previous studies at MIT have shown very promising results with iridium as a candidate inert anode material [7;8;22]. Therefore, a main goal of this study was to continue research into the plausibility of an inert iridium anode at a larger scale, and as a function of process parameters.

Anodes were constructed of 99.9% pure iridium obtained from Furuya Metal Co., Japan. The iridium was received in 100mm x 100mm x 1mm sheets. Iridium is very hard and brittle, and has a very high melting temperature, 2446°C [23]. Therefore, fabrication is not possible with traditional machining or casting methods. However, success was enjoyed by fabricating the anodes using a CNC waterjet cutting machine and GTAW welding methods.

The most common anode geometry was 30mm x 10mm x 1mm bars. The anodes were cut from as-received iridium sheets and welded to a 1/8" diameter molybdenum lead wire. The wire was then sheathed in a 1/8" internal diameter, 99.8% alumina tube from McDanel Advanced Ceramics to protect the molybdenum from oxygen evolved during electrolysis. The bottom of the tube was then sealed to the molybdenum/iridium interface with alumina-based refractory paste to prevent any exposure of the molybdenum. This was done not only to prevent corrosion of the molybdenum, but to also prevent the consumption of evolved oxygen by the molybdenum, as the exhaust was analyzed using gas chromatography to calculate anodic current efficiency.

2.1.2.1.1.1 Unique Morphologies

Iridium is a very expensive material to conduct research with due to not only the high cost of the metal itself, but the increased labor costs associated with the difficulty of machining the material. Because of this, experimenting with unique morphologies was difficult using the humble machining capabilities at MIT. However, MIT was afforded a unique opportunity to work with Plasma Processes, a company from Birmingham, Alabama that specializes in state-of-the-material and coating fabrication.

Researchers from Plasma Processes collaborated with the author on NASA's lunar oxygen production project as part of an SBIR grant that the company received to research anode fabrication techniques. Plasma Processes manufactured the following anodes using a proprietary molten salt electrodeposition process:

- Iridium-coated graphite – this anode was made from a graphite disc, on which a thin (~1mm) coating of iridium was deposited. Final geometry: 13mm height x 50mm diameter disc.
- Porous disc anode – this anode was a porous disc of iridium. Pore size was on the order of 1mm. Final geometry: 13mm height x 50mm diameter disc.



Figure 2.3: Three iridium anodes made by Plasma Processes using a proprietary molten salt electrodeposition process. Left: "Wagon Wheel" anode showcases the ability of the process to deposit solid iridium in unique geometries. Tests with this anode not discussed in this study. Middle: A graphite disc coated with ~1mm of iridium. Right: A porous iridium anode with pore on the order of 1mm. The pores in this photograph are clogged with entrained electrolyte left over from a previous submersion test.

Both of these anodes offered a unique opportunity to test possible engineering solutions to problems associated with the high costs of iridium. Each anode represented different routes that could be investigated to stretch the amperage available per pound of iridium metal used in an MOE cell.

2.1.2.1.2 Other Anode Materials

In addition to the ground-up scientific research aimed at creating the perfect inert anode material, an exhaustive investigation of commercially available refractory electrode materials was necessary. The most obvious application for high temperature electrodes is furnace heating elements. Therefore, vendors of heating elements were primary source to obtain these materials. Among these materials can be found an everyday application of an oxide passivated metal (refer to section 1.2.2.2) called molybdenum disilicide (MoSi_2), used for electrical resistance heating. Molybdenum disilicide is an alloy of two readily oxidized metals. However, it is virtually impervious to corrosion in oxidizing atmospheres up to 1800°C [24]. This excellent corrosion resistance is due to silicon preferentially oxidizing and forming a protective SiO_2 layer, which protects the metallic substrate from exposure to the oxidizing environment.

2.1.2.2 Cathode

Except for experiments involving novel crucible designs (refer to section 2.1.2.3.2), all experiments were conducted using 50mm diameter x 2mm thick molybdenum disc cathode. In all experiments, the cathode was located below the anode in the cell. Molybdenum was selected, despite its susceptibility to oxidation, because the cathode was covered by slag and always located below the anode in the cell. Therefore, the cathode would never come in contact with the evolving oxygen bubbles or the oxygen-containing atmosphere of the furnace during electrolysis. Furthermore, the cathodic potential should offer protection from oxidation during electrolysis. The cathodes were machined from 1mm thick molybdenum sheets using a CNC waterjet cutter. Two 1mm thick discs were then stacked tightly together and secured to a 36" long x 0.125" diameter threaded molybdenum rod using molybdenum nuts.

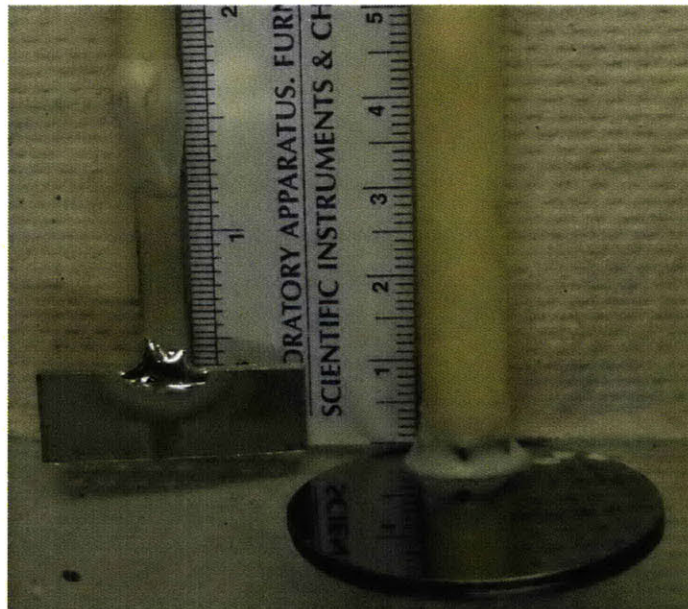


Figure 2.4: Iridium anode and molybdenum cathode before electrolysis.

2.1.2.3 Crucibles

As mentioned above, the length of experiments was usually determined by the maximum service life of the crucible. Therefore, determining appropriate crucible material became a vital task in order to perform repeatable experiments. In smaller scale MOE studies at MIT, standard high purity alumina crucibles (99.8% Al_2O_3 from McDanel Advanced Ceramics) were preferred, based on a cost-benefit analysis [8]. However, as experimental times became longer, it was soon realized that alumina crucibles were only reliable as slag containers for a maximum of 5 hours above 1550°C . Furthermore, as studies began on different slag chemistries, it was found that crucible performance was greatly affected by the basicity of the slag.

An obvious alternative for ceramic crucibles is the refractory metals (Mo, W, Ta, etc.). These materials were initially avoided due to their susceptibility to oxidize. This was a concern for two reasons. First, it was a concern that the extremely high temperatures would cause runaway oxidation and catastrophic failure. Second, the refractory metals would absorb the electrolytically produced oxygen, leading to false current efficiency measurements. However, it was found that molybdenum crucibles, despite severe oxidation, would last considerably longer than their ceramic counterparts. Furthermore, while the second concern does present an issue when determining current efficiency with respect to oxygen concentration of the furnace exhaust, it is not an issue when current efficiency is determined by concentration of iron in cathodic product; which is a more useful metric for current efficiency measurements for the iron production project.

2.1.2.3.1 Effect of Electrolyte Basicity on Crucible Selection

Working with molten oxides presents unique challenges with regard to refractories, as slags tend to be strong solvents of traditional ceramic refractory materials. Silicates in particular are miscible with most other oxides, and it was understood from the beginning that quartz would be useless as a containment material for any molten oxide system. Furthermore, because of this property, silicate systems will also tend to dissolve through most commonly used ceramic

crucible materials if given enough time.

When studies began with slags of varying composition, it was found that an alumina crucible, which could normally withstand up to 4 hours at MOE operating temperatures with a silicate slag, would be completely dissolved by its contents within an hour when used with a highly basic, calcia-rich slag. Similar to aqueous systems, basic slags will tend to dissolve acidic oxides faster, and vice versa. Therefore, one must take into account optical basicity of the slag when determining the appropriate crucible material. With this taken into account, it was found that silica-free, calcia-rich slags with high optical basicity will be successfully contained in a magnesia (MgO), a basic oxide, for very long times (>10 hours). Conversely, it was found that relatively acidic silicate slags will dissolve magnesia faster than alumina, a slightly acidic oxide.

2.1.2.3.2 Novel Crucible Design

Using the cathode described above has several disadvantages. It is very difficult to perform postmortem analysis on the cathodic product of a molybdenum cathode. The cathode must be lifted out of the electrolyte while still molten to prevent it from becoming permanently encased in the oxide glass that forms upon cooling. If there was a well segregated liquid iron pool on the cathode, the lifting of the cathode causes the molten phases to mix. One is left with an agglomeration of slag, partially oxidized iron-molybdenum alloy, and small porosities on the cathode for analysis. This makes it extremely difficult to determine the morphology of the deposited iron pool and the purity of iron contained therein.

In addition to causing a difficult postmortem analysis, the lead wire necessary for the disc type cathode can fail. MOE experiments can be very complicated, expensive, and extremely vulnerable to failure of any link in the chain. Therefore, it is extremely important that any diagnosis of possible failure mechanisms be remedied whenever possible. Current is fed to the cathode by 1/8" molybdenum rod. Due to the furnace's design, all electrical and gas connections must come in through the furnace cap. Therefore, the current lead to the cathode must run past the anode and through the electrolyte. In order to prevent short-circuiting, as well as protect the

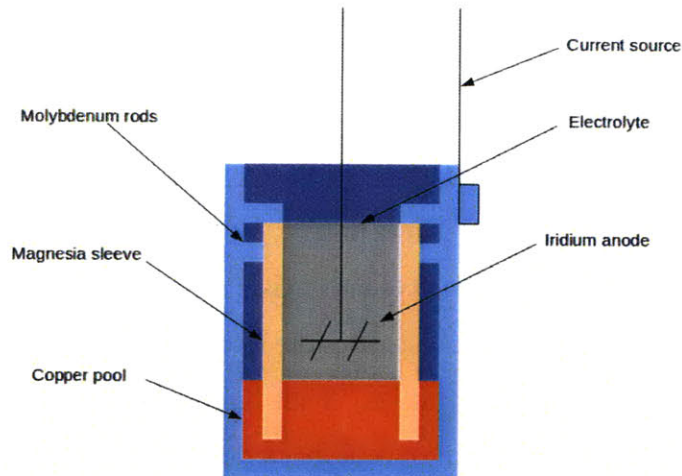


Figure 2.5: Novel crucible design to circumvent shortcomings of disc cathodes.

molybdenum rod from oxidation, it is sheathed in a ceramic tube. However, as stated above, the molten electrolyte can eat through the ceramic. And, when this happens, the molybdenum is exposed to oxygen and quickly oxidizes, causing it to lose its electrical conductivity.

In order to circumvent these disadvantages, a novel crucible design which eliminates the need for a molybdenum disc cathode has been tested. The design uses a molybdenum crucible, which is connected to the current supply and supplies cathodic potential to the electrolyte by means of a molten copper pool. Copper was chosen for two main reasons:

- It has low miscibility with both iron and molybdenum
- It is more dense than iron, allowing iron to float on top of it

Because of these two key characteristics, the copper pool will allow there to be 3 well segregated strata of copper, iron, and electrolyte. Faradaic reduction reactions take place at the copper/electrolyte interface and a ceramic sleeve keeps the current lines directed vertically down. A cross-sectional model of this crucible design is shown in Figure 2.5.

2.2 Electrolyte Selection

The electrolyte composition for studying MOE as a method to produce oxygen on the moon is fixed by the composition of lunar regolith (refer to section 1.1.2). Conversely, the electrolyte for terrestrial iron production can be selected to best fit the criteria listed in section 1.2.3. Therefore, three electrolytes were used throughout this research (Table 2.2). The first two of these three electrolytes were based on the composition of lunar regolith (minus the highly volatile oxides), whereas the third composition was selected to most closely meet the criteria listed in section 1.2.3.

Table 2.2: Properties of different slags used in this study.

Slag	SiO ₂	CaO	MgO	Al ₂ O ₃	FeO	Fe ₂ O ₃	T _m (°C)	Viscosity (Pa.s)	Density (g.cm ⁻³)	Conductivity (S.cm ⁻¹)	Melt basicity
Lunar	45.6	19.1	23.6	11.7	X	-	1311	~1	~2.7	~0.2	0.606
Iron1	45.6	19.1	23.6	11.7	-	X	1311	~1	~2.7	~0.3	0.606
Iron2	-	57.9	10.3	31.8	-	X	1400	~0.27	~2.7	~0.6	0.753

Chapter 3: Experimental Results

3.1 Iridium

3.1.1 Electrodeposited Iridium Anodes

The electrodeposited anodes were tested in the smaller Mellen furnace with a 4.0" ID x 30" L 99.8% furnace tube from McDanel Advanced ceramics. The iridium-coated graphite and porous iridium anodes were tested as feasible means to utilize unique morphologies to circumvent the high capital costs associated with using iridium as an inert anode material. Both anodes were tested with similar process parameters, which are detailed in Table 3.1.

Table 3.1: Parameters of experiments performed with electrodeposited iridium anodes.

Anode Tested	Ir-Coated Graphite Anode	Porous Ir Anode
Electrolyte	LUNAR (Table 2.2)	LUNAR (Table 2.2)
Atmosphere	Vacuum-assisted (100 Torr) purge with Ar X 5 + vacuum-assisted (100 Torr) purge with He X 5 + 300 ml/min He flow rate	Vacuum-assisted (100 Torr) purge with Ar X 5 + vacuum-assisted (100 Torr) purge with He X 5 + 300 ml/min He flow rate
Power Supply and Data Acquisition	PARSTAT 2273 w/ KEPCO 20A/20V Power Booster	Sorensen 25A/40V Power Supply with Multimeters and Camera, PARSTAT 2273 w/ KEPCO 20A/20V Power Booster
Small Mellen Furnace Program ²	100°C/hr to 1675°C, dwell @ 1675°C 7 hours, 100°C/hr to 25C	100C/hr to 1675°C, dwell @ 1675°C 5 hours, 100°C/hr to 25C

Unfortunately, time constraints and faulty equipment effected the quality of electrochemical data collected for experimentation with the iridium-coated graphite anode. However, the primary goal for testing this anode was whether or not iridium coating would effectively protect the graphite substrate and if the ~1mm coating would last during electrolysis.

In most MOE tests, the cathode area was substantially larger than the anode area. This was to force the limiting current density to be on the anode rather than the cathode. However, the large

² Values reported are PVs, please refer to section 2.1.1 for explanation of temperature gradient during experiments.

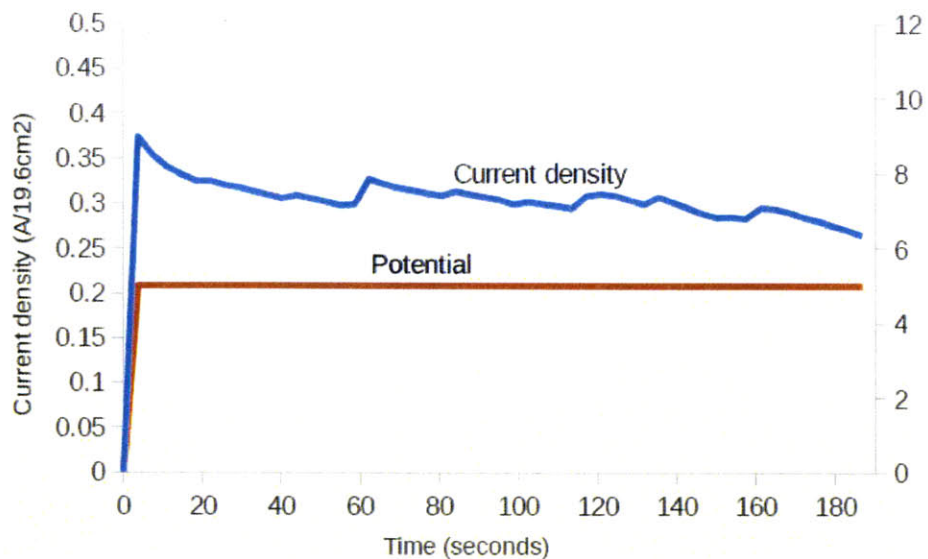


Figure 3.1: Electrolysis data for iridium-coated graphite anode.

size of the electrodeposited anodes and the limited size of the furnace dictated the maximum size of the cathode. Therefore, the cathode for both experiments was a disc measuring 50mm diameter x 0.25mm thick. Details about the anodes used can be found in section 2.1.2.1.1.1.

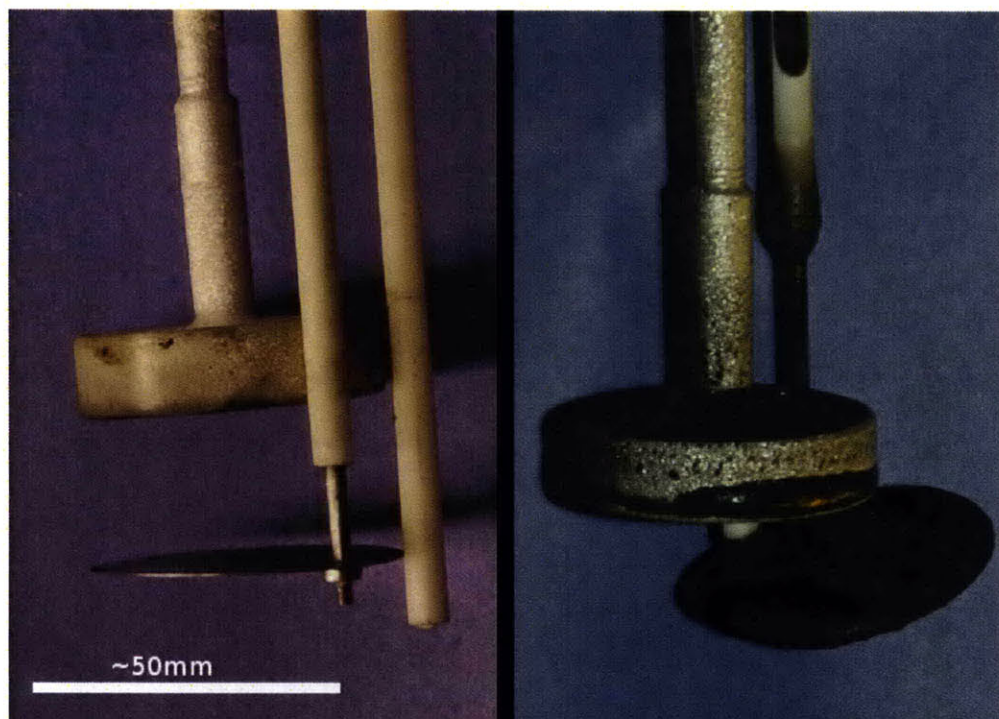


Figure 3.2: Iridium-coated graphite anode before (left) and after (right) electrolysis.

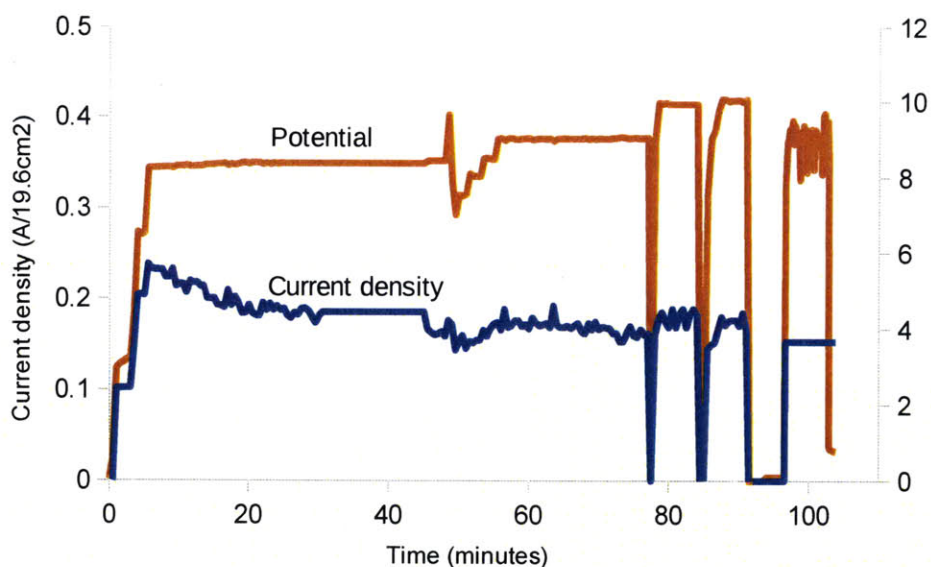


Figure 3.3: Electrolysis data for porous iridium anode.

As mentioned above, the data acquisition for the iridium-coated graphite anode was flawed due to faulty equipment. The reason is unknown, but after a 4 hour electrolysis experiment only approximately 3 minutes of data was recorded by the potentiostat. However, the author did take notes during the experiment which record that the current response to the potentiostatic

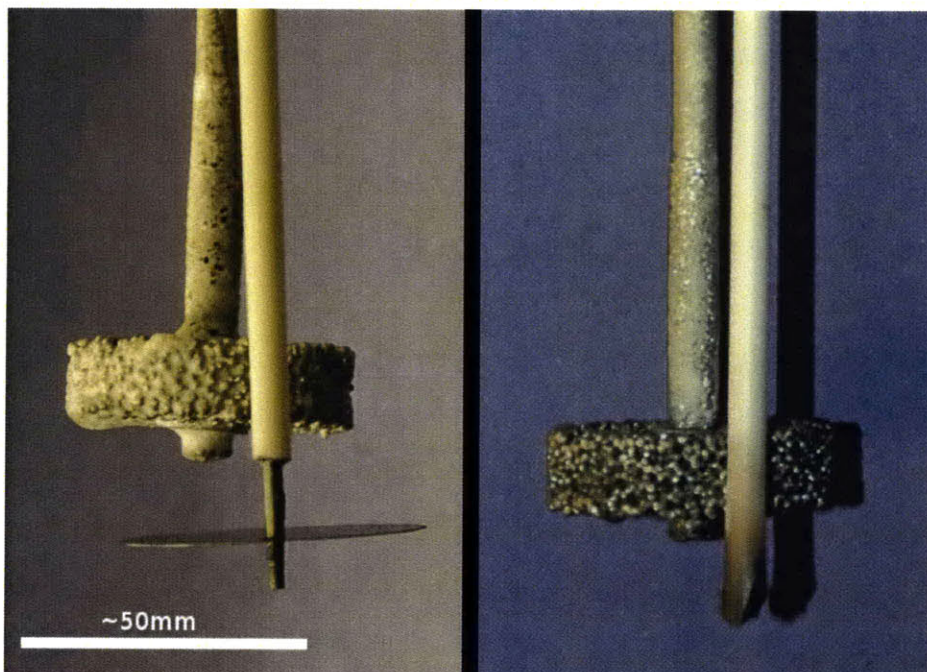


Figure 3.4: Porous iridium anode before (left) and after (right) electrolysis.

experiment eventually leveled out at approximately 8A (current density of approximately 0.4 A/cm²).

Because of problems with the PARSTAT in the experiment with the iridium-coated graphite anode, a manual power supply, multimeters, and a digital camcorder were acquired as contingency for data acquisition. Unfortunately, problems with the PARSTAT continued to plague the experiment. Therefore, the author had to watch the video recording of the multimeters and manually record thousands of current and potential data points to fill in holes not recorded by the PARSTAT.

The experiment with the porous anode was planned for 4 hours, but stopped after 103 minutes due to high cell voltages (>10V) and poor current response (~0.15 A/cm²). It was thought that the poor data may be caused by crucible failure. However, it turned out the poor conduction was an artifact of the anode morphology. As mentioned above, the high silica slags are very viscous, even at temperatures above 1550°C, due to the networks formed by bridging oxygens in the silica. Therefore, gaseous bubbles, such as those formed during oxygen evolution, become very easily trapped at obstacles such as the pores in the porous anode. While a porous anodes will have a much larger surface area, the pores need to be much larger than ~1mm for silicate slags in order for them to increase faradaically active surfaces. In this case, the small pores are believed to have done just the opposite and reduce faradaically active surface area with trapped oxygen gas.

3.1.2 Effect of Electrolyte Basicity on Iridium Anodes

Preliminary results from experiments using iridium anodes with the very basic IRON2 slag seemed contradictory to the years of research already performed at MIT. Iridium anodes, which seemed to qualify as inert in lunar regolith simulants, such as the electrolyte LUNAR, were dissolving entirely during electrolysis in IRON2. The ionic conduction mechanism in molten oxide electrolytes dictate that higher conduction requires high optical basicity. Energy requirements of MOE are a function of electrolyte conductivity and have huge implications for

the feasibility of MOE for iron production. Therefore, it was necessary to determine why iridium seemed to work in silicate slags but not in very basic, calcia-rich slags, such as IRON2.

Table 3.2: Parameters of experiment on effect of electrolyte basicity.

Anode Tested	30mmx10mmx1mm Ir Plate	30mmx10mmx1mm Ir Plate
Electrolyte	IRON1 (Table 2.2)	IRON2 (Table 2.2)
Atmosphere	Vacuum-assisted (100 Torr) purge with Ar + 300 ml/min Ar flow rate during experiment	Vacuum-assisted (100 Torr) purge with Ar + 300 ml/min Ar flow rate during experiment
Power Supply and Data Acquisition	PARSTAT 2273 w/ KEPCO 20A/20V Power Booster	PARSTAT 2273 w/ KEPCO 20A/20V Power Booster
Carbolite Furnace Program ³	100°C/hr to 1600°C, dwell @ 1600°C 7 hours, 100°C/hr to 25°C	100C/hr to 1600°C, dwell @ 1600°C 7 hours, 100°C/hr to 25°C

A study was performed to determine the effect of optical basicity on the inertness of iridium anodes. Experiments were conducted using iridium anode plates (30mm x 10mm x 1mm described in section 2.1.2.1.1) in IRON1 and IRON2 electrolytes, with all other process parameters constant (Table 3.2).

Identical iridium anodes were subjected to identical conditions in MOE experiments. Galvanostatic electrolysis was conducted at 3.5A with an anode/cathode distance (ACD) of 20mm for 4 hours; the anodes were then raised out of the electrolyte to cool. After the

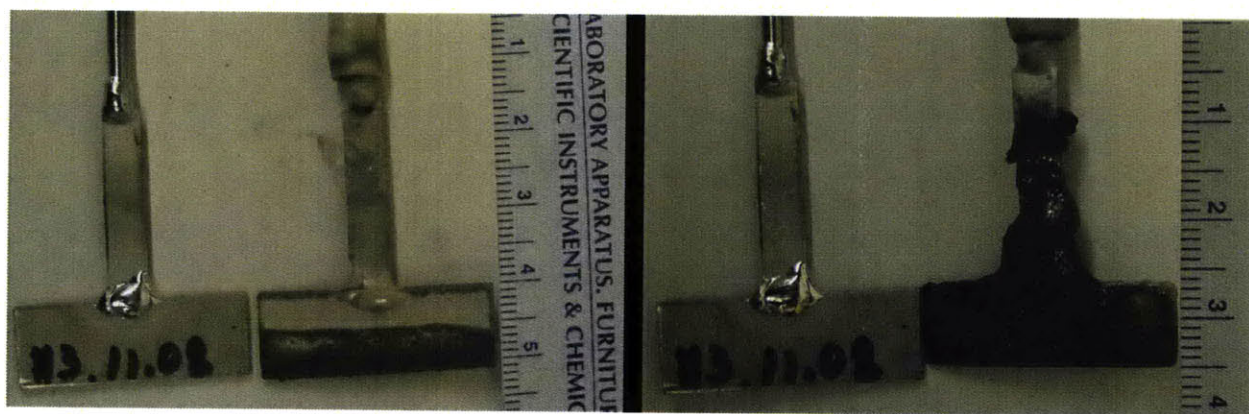


Figure 3.5: LEFT: Before (left) and after (right) of iridium anodes used for MOE in Iron1. RIGHT: Before (left) and after (right) of iridium anodes used for MOE in Iron2.

³ Values reported are PVs, please refer to section 2.1.1 for explanation of temperature gradient during experiments.

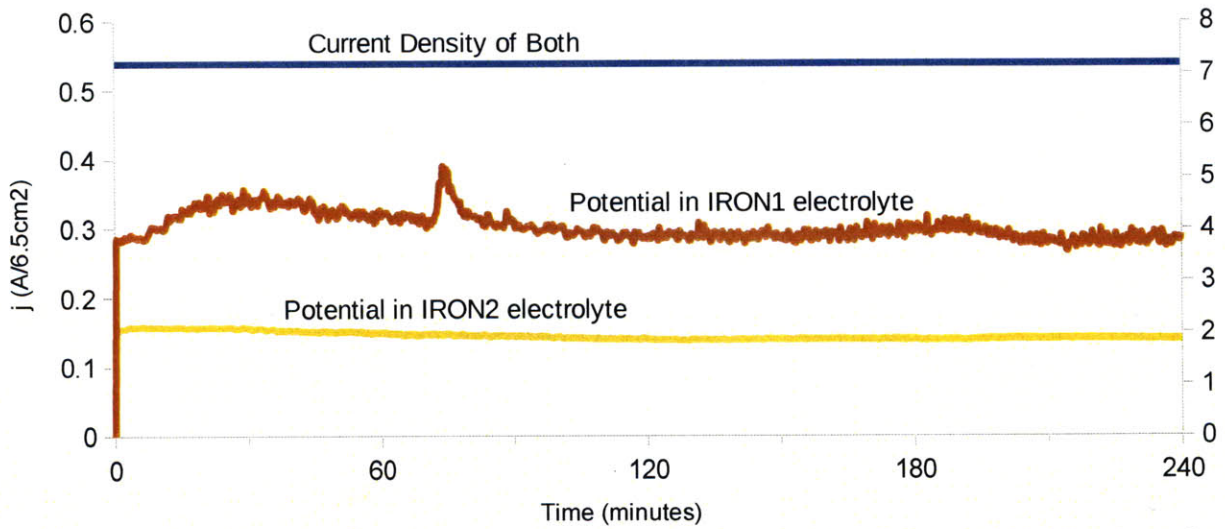


Figure 3.6: Electrolysis data for study on effect of electrolyte basicity; notice the effect of electrolyte composition on potential response to the same constant current density.

experiment, anodes were measured, weighed, and analyzed using SEM and SEM/EDAX. As can be seen in Figure 3.5, the anode subjected to IRON2 electrolyte (RIGHT) sustained much more severe loss of material.

The data in Figure 3.6 show that the much more basic slag (IRON2) requires about half the potential for a given current response. This difference in potential response among the two electrolytes correlates nicely with the theoretically determined conductivities of the two slags;

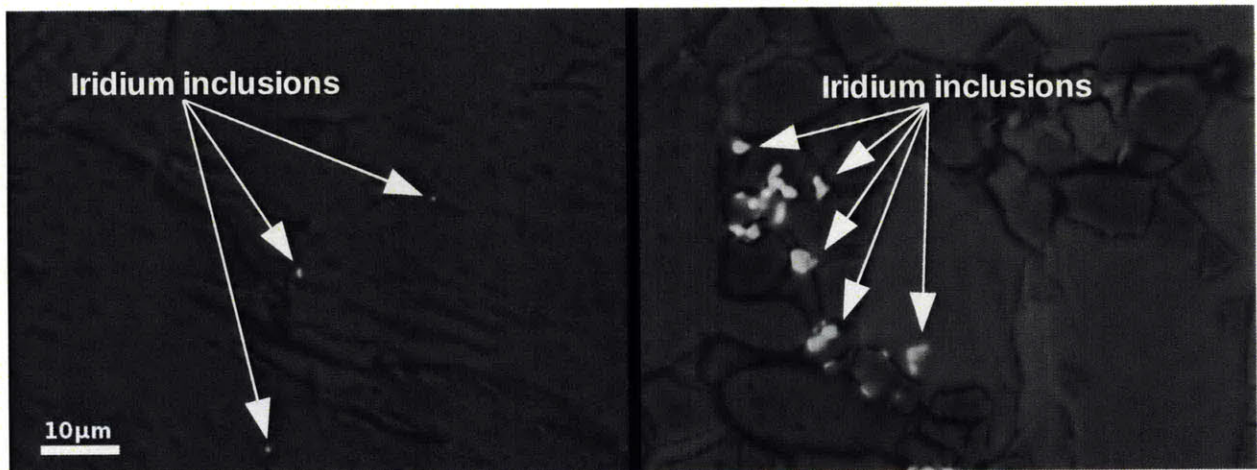


Figure 3.7: Representative back-scattered electron micrographs of bulk electrolyte after electrolysis for experiments done in IRON1 (left) and IRON2 (right). Both electrolytes contained inclusions of iridium metal believed to have dissolved as IrO_2 and then decomposed to pure metal while in the electrolyte.

IRON2 has about twice the conductivity of IRON1 due to its high basicity.

Upon analyzing the bulk electrolyte after electrolysis, iridium metal inclusions are easily identified using back-scattered electron microscopy (BSE). As one can see in Figure 3.7, the IRON2 electrolyte (right) has far more iridium metal contained in the slag, which directly correlates with the increased consumption of the anode seen in Figure 3.5. These inclusions show up as a high contrast phase and were identified as iridium metal by using an energy-dispersive X-ray spectroscopy enabled scanning electron microscope (SEM/EDAX). Average EDAX analysis of 10 spots indicates that the inclusions are greater than 50% iridium and less than 17% oxygen (the balance being cations of the other constituent oxides). Therefore, by this measurement, the particles must be at least partially iridium metal. The small size of the inclusions, especially in the IRON1 electrolyte, and the inherent shortcomings of EDAX with regard to correctly quantifying concentrations of light elements, makes it difficult to measure precise chemical composition of the inclusions. However, the high contrast of the phase corresponds to what one would expect to see of a metal when using SEM, and iridium is the only metal that should exist at that position in the electrolyte, midway between the anode and the cathode.

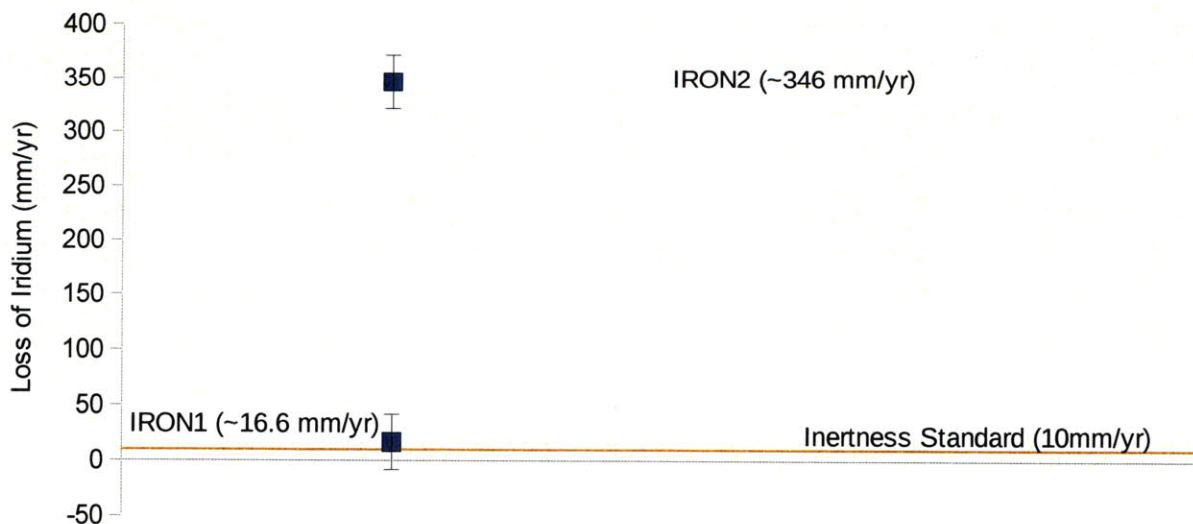


Figure 3.8: Calculated loss of iridium per year for IRON1 and IRON2, based on weight loss measurements from electrolyte basicity experiments.

3.1.3 Results from Novel Crucible Design

The novel crucible design schematic is shown in Figure 2.5. The design was tested using the experimental parameters detailed in Table 3.3.

Table 3.3: Experimental parameters for novel crucible tests.

Anode Tested	30mmx10mmx1mm Ir Plate Cross (FIGURE)
Electrolyte	<i>Similar to IRON1 (Table 2.2)</i>
Atmosphere	300 ml/min Ar flow rate during experiment with overnight purge.
Power Supply and Data Acquisition Carbolite Furnace Program ⁴	ARGANTIX XDS Power Supply and Data Acquisition 100°C/hr to 1750°C, dwell @ 1750°C 7 hours, 100°C/hr to 25°C

The scope of these tests was to determine whether or not this new crucible design would prove useful for laboratory-scale MOE tests as a means to increase quality of cathodic product. The electrolyte used for this experiment was similar to IRON1, except that electrolyte contained magnetite (Fe_3O_4) instead of hematite (Fe_2O_3), and was slightly more basic due to increased calcia concentration. Magnetite was used in order to test MOE using a common ore.

There were slight concerns as to whether or not the metallic layers would cause a thermoelectric effect or noise caused by induction. However, the electrolysis data collected from the potentiostatic experiment are what one would expect from an MOE experiment. The current response corresponds to an electrolyte conductivity of approximately 0.2~0.3 S/cm with an ACD of 2~3 cm, which is what was used in the experiment shown in Figure 3.9. Furthermore, the perturbation of the current signal is expected; it is believed to be caused by arrested oxygen evolution due to high viscosity of silicate electrolytes.

Figure 3.10 is a picture taken of the electrolyte after electrolysis. A rough calculation of estimated iron product from total charge passed during the experiment (assuming cathodic current efficiency of 30%) predicts that there should on the order of 0.1~0.4mm of iron metal

⁴ Values reported are PVs, please refer to section 2.1.1 for explanation of temperature gradient during experiments.

Table 3.4: Experimental parameters for novel crucible tests.

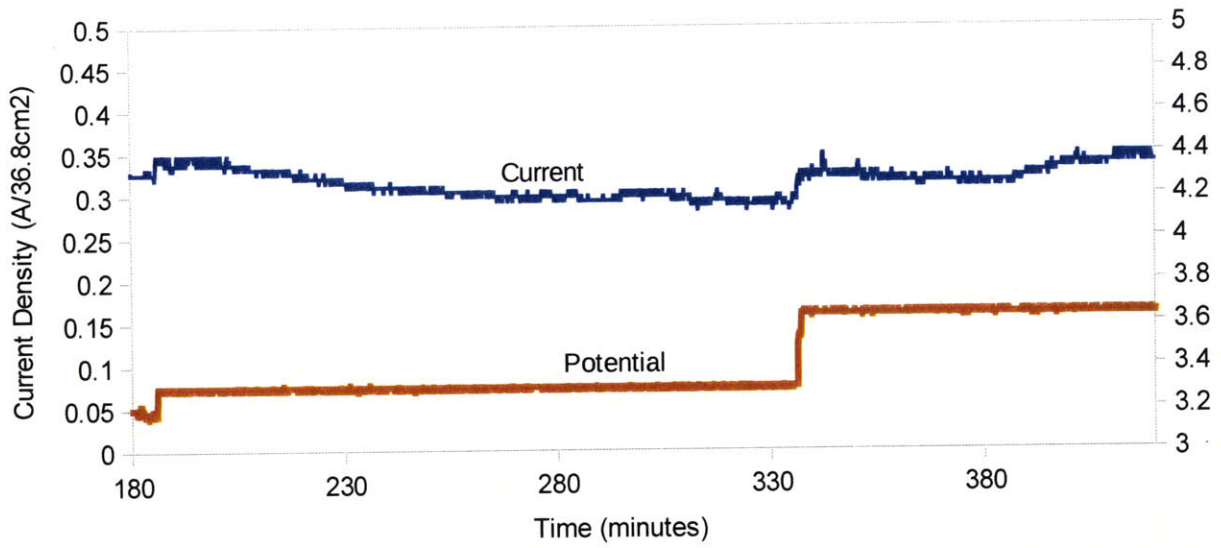


Figure 3.9: Electrolysis data from novel crucible design experiment.

deposited at the cathode. While roughly that amount of iron was found at the cathode, it did not deposit as one continuous pool of iron. As one can see in Figure 3.10:2, the iron is in the form of small beads. It is thought that these beads are the result of nucleation sites coalescing due to surface tension effects as more iron metal is produced. Therefore, a longer experiment should

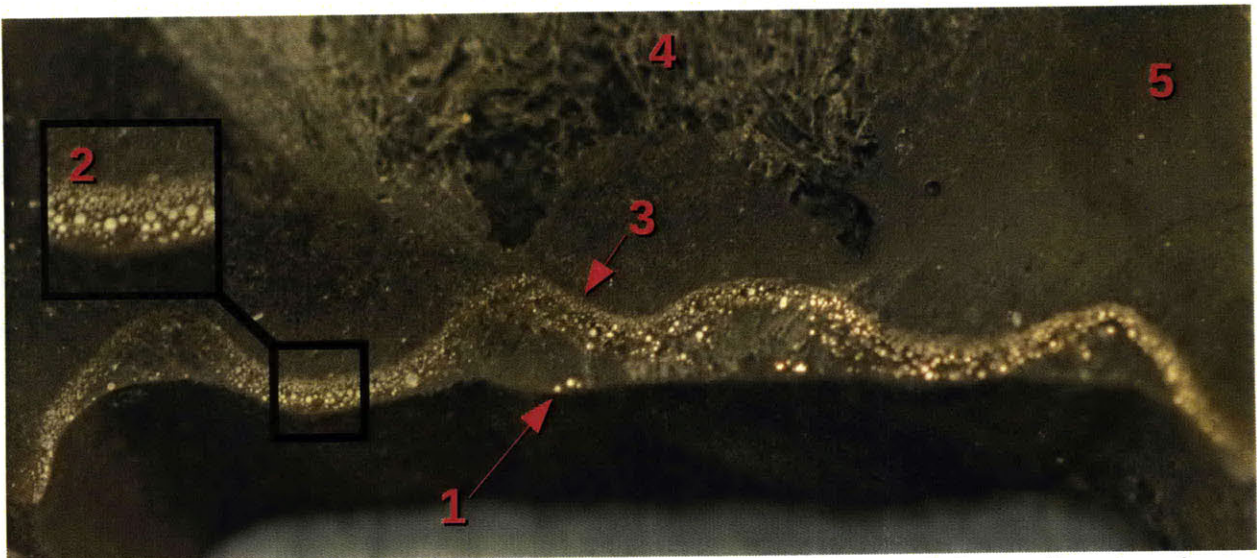


Figure 3.10: Electrolyte after experiment with novel crucible design. 1: Copper/iron interface. 2: 2X magnification of iron beads produced at cathode. 3: Iron/electrolyte interface. 4: Pores in electrolyte caused by trapped oxygen gas. 5: Bulk electrolyte.

result in a continuous pool of iron. However, as mentioned above, the total length of the experiments are currently dictated by the service life of the ceramic refractories.

SEM/EDAX confirmed that the metallic beads in the cathodic product are iron metal. Due to the morphology of the iron, the iron beads are contained in a matrix of slag and small concentration of iridium. The iridium metal at the cathode presumably settled out of the electrolyte due to its high density. However, it is also possible that some of the iridium found its way to anode via a mechanism similar to electro-refining (i.e. oxidized at the anode into solution and reduced back into metal at the cathode).

3.2 Other Candidate Anode Materials

Due to the prohibitively high cost of iridium, MOE will likely never be a feasible process for industrial-scale iron production unless a different anode material can be identified. While the egregious operating environment associated with MOE will likely require a ground-up materials engineering approach, an exhaustive survey of several commercially available high temperature electrode materials was conducted. The results of this search are listed in Table 3.5.

While a suitable anode material was not discovered during this study, several key lessons were learned from the endeavor. This study highlighted the difficulties associated with using ceramic materials as electrolysis anodes. The first major drawback of using a ceramic is the poor thermal shock resistance of the material. In a realistic, industrial-scale cell the anode will have to be capable of being submerged and withdrawn from the molten electrolyte without failure. In terms of energy-budgeting, a plant will keep the absolute minimum volume of the cell at operating temperatures, meaning the anode will likely travel through large temperature gradients during deployment. The tin oxide experiments demonstrated very well the poor thermal shock resistance of ceramics, as none of the tin oxide anodes survived long enough to even attempt electrolysis.

The second major shortcoming of ceramics was highlighted by electrolysis with lanthanum chromate. Lanthanum chromate has much better thermal shock resistance than tin oxide. Lanthanum chromate is a well known resistance heating element material (it is used for the

heating elements in the Carbolite furnace used for MOE studies at MIT). Therefore, it was elected as a candidate material due to its known high-temperature stability and corrosion resistance. However, this ceramic is a poor conductor in terms of electrolysis anode materials, and would require cell voltage far too high for a profitable industrial-scale cell. In fact, the

Table 3.5: Results of survey conducted on commercially available, high-temperature electrode materials as MOE anode candidates⁵.

Experimental parameters constant for all materials.		
Furnace Profile	Electrolyte	Atmosphere
100°C/hr to 1700°C, dwell @ 1700°C for 8 hours, 100°C/hr to 25C	IRON2	He flow rate of 1 L/min during ramp-up and experiment
Material	Material Type	Performance
Molybdenum	Metal	As predicted, molybdenum rapidly oxidized and was lost due to volatility, as well as solubility in electrolyte, of the molybdenum oxides. ~93 gram anode lasted almost 2 hours at 0.88A/cm ² , and produced several grams of iron alloyed with molybdenum at the cathode.
Graphite	Non-metal	As expected, the graphite began violent carbothermic reduction of the iron oxide upon submersion. Electrolysis was conducted at ~1A/cm ² for 3 hours. Experiment produced several grams of iron in cathodic product. However, it is most likely that the majority of this iron was produced carbothermically.
Molybdenum Disilicide	Oxide-passivated metal	Molybdenum disilicide forms a silica passivation layer. However, because of silica's high solubility in IRON2, it is believed the oxide layer was quickly dissolved, exposing the molybdenum. Despite its overall failure, MoSi ₂ was the most promising material of the survey, producing ~25 grams of iron after 2 hours at 0.89A/cm ² .
Lanthanum Chromate	Ceramic	LaCrO ₄ readily dissolves in IRON2, even when tested without electrolysis. Electrolysis was performed for almost 2 hours before dissolution of the anode. However, a cell voltage of nearly 30V was required to obtain a current density of 0.28A/cm ² .
Tin Oxide	Ceramic	Anode fractured during heat up due to extremely poor thermal shock resistance. Because of this, no experiment has ever reached electrolysis. This material would likely never be a candidate for any industrial scale, high-temperature electrolysis, as thermal shock resistance decreases with size.

⁵ The results listed in Table 3.5 are from research conducted by Hojong Kim and Shuqiang Jiao, postdoctoral associates of the author during his graduate studies at MIT.

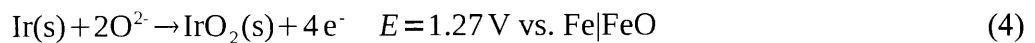
electrolysis test performed with a lanthanum chromate anode required nearly a 30V cell potential (ACD=2cm) to produce a 0.28 A/cm² current density on the anode. An industrial MOE cell will probably require a current density of about 1 A/cm² or greater in order to achieve realistic production requirements. Using lanthanum chromate at those current densities would likely require over 100V, which would be far too much for a profitable MOE cell.

Chapter 4: Implications of Experimental Results and Future Considerations

4.1 Proposed Corrosion Mechanism for Iridium Anodes

Despite the fact that iridium is the most chemically stable of all elements, its superior performance as an inert anode material during MOE is thought to be the result of an entirely different set of mechanisms. Rather than resisting corrosion due to the metal's very low reactivity, it is believed that the iridium anodes endure due to kinetic equilibrium between the oxidizing anodic potential and iridium oxide's propensity to spontaneously decompose at high temperatures. In fact, since this is a combination of competing electrochemical and redox reactions, the iridium isn't "stable" at all.

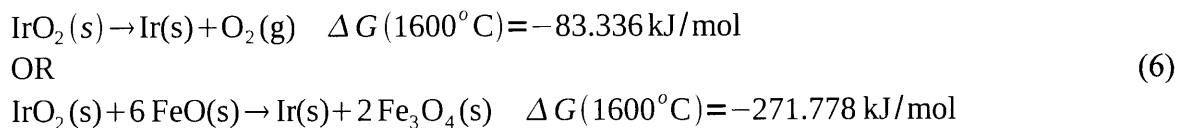
In order to understand this proposed mechanism, we must first discuss the possible reactions iridium can participate in during electrolysis. Iridium will oxidize at the anode by the following reaction [25]:



The molten oxide electrolyte is an excellent solvent for other oxides. Therefore, iridium oxide produced by the anodic potential can be dissolved by the electrolyte:



However, once the iridium is dissolved and travels away from the anodic potential, the iridium oxide is no longer stable and will spontaneously decompose via one of the following redox reactions [18]:



If reaction (6) occurs before the iridium oxide travels a certain distance away from the anode the

iridium metal will be preferentially adsorbed back onto the anode's due to surface tension effects. Reactions (4), (5), and (6) are driven by independent forces. Therefore, for the sake of a thought experiment, we may arbitrarily assign theoretical rates to each of these reactions:

$$R_{\text{anode}} = \text{rate of oxidation of Ir to IrO}_2 \text{ in units of } \frac{\text{mol Ir}}{\text{s}} \quad (7)$$

$$R_{\text{dissolve}} = \text{rate of dissolution of IrO}_2 \text{ in units of } \frac{\text{mol IrO}_2}{\text{s}} \quad (8)$$

$$R_{\text{redox}} = \text{rate of decomposition of IrO}_2 \text{ to Ir in units of } \frac{\text{mol IrO}_2}{\text{s}} \quad (9)$$

We may then use these theoretical rates to determine how each of these reactions will effect the loss of iridium from the anode into the slag. The way that iridium would be lost into the slag would be by the dissolution of iridium oxide, formed in reaction (4), into the slag by reaction (5). However, because these reactions have independent driving forces, reaction (6) will occur simultaneously to reaction (5), which will “save” some of the iridium from being lost to the slag. Because reactions (5) and (6) have reactants which must come from the product of reaction (4), we know that the total rate of iridium metal lost will be limited to the rate of reaction (4). Furthermore, because reactions (5) and (6) result in the loss or retention of iridium, respectively, and occur simultaneously, the total amount of iridium lost will be proportional to a weighted average of these two reactions. Therefore, we arrive at the following theoretical model:

$$R_{\text{lost}} \left(\frac{\text{mol Ir}}{\text{s}} \right) = R_{\text{anode}} \frac{R_{\text{dissolve}}}{R_{\text{dissolve}} + R_{\text{redox}}} \quad (10)$$

The proposed mechanism for the corrosion of iridium anodes in an MOE cell are illustrated in Figure 4.1. Unfortunately, the operating conditions of an MOE cell cause reactions (4), (5), and (6) to always move to the right, as written. Therefore, there will always be some loss of iridium by this mechanism. However, if $R_{\text{redox}} \gg R_{\text{dissolve}}$ then $R_{\text{lost}} \rightarrow 0$.

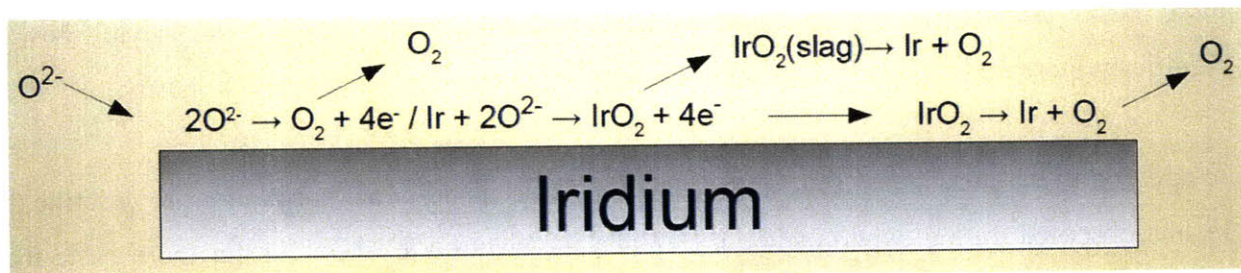


Figure 4.1: Model of proposed mechanism for the inertness of iridium.

While this mechanism has not yet been proven empirically, there is qualitative evidence from the experimental results in the previous chapter that corroborate this proposal. In order to explain this correlation, we must first discuss the effect of experimental parameters on the rates give in equations (7-9). We know that R_{anode} is driven by the anodic potential. Therefore, the rate of iridium oxidized is a function of anodic current density:

$$R_{anode} = f(j) \quad (11)$$

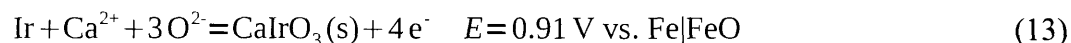
As described in section 1.2.3.1, elements with higher oxidation states and larger electronegativities will form oxides with higher optical basicity. Therefore, by this logic, one can easily realize that iridium, which forms Ir(IV) oxide and has an electronegativity of 2.20, would form a very acidic oxide. Basic oxides tend to be better solvent for acidic oxides, and vice-versa; this is directly analogous to aqueous systems. Therefore, one can see that the extent, and very likely the rate, at which iridium oxide will dissolve in a molten oxide electrolyte will be a function of the electrolyte's optical basicity:

$$\text{formula } R_{dissolve} = f(\Lambda_{electrolyte}) \quad (12)$$

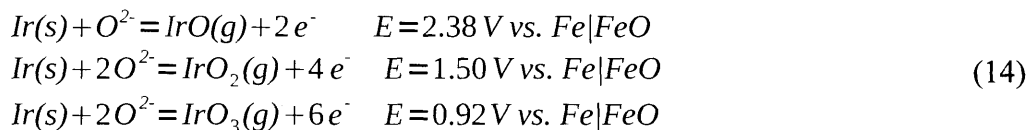
MOE experiments performed in this study show a direct correlation between iridium anode stability and these two process parameters (i.e. anodic current density and electrolyte basicity). Iridium anodes will exhibit inertness, less than 10mm/yr recession rate, with a current density no greater than 0.5A/cm² when used in relatively acidic electrolytes, such as LUNAR and IRON1. However, as shown in section 3.1.2, identical experiments conducted in two electrolytes of different optical basicity resulted in a significant increase in loss of anode material when using a

more basic electrolyte. Furthermore, similar experiments in IRON2 electrolyte show a significant increase in iridium loss during electrolysis with high anodic current density.

In addition to the mechanism state above, there have been additional postulations to describe the results observed during experimentation. While the electrolyte IRON2 is far more basic than IRON1, which should make it a stronger solvent for IrO₂, it also has a high concentration of calcia. Calcia is known to form calcium-iridates [26]. An example of this reaction is:



Therefore, it is likely that the formation of this iridate is partially responsible for the accelerated anode corrosion in IRON2. Additionally, iridium is well known to form volatile oxides. Possible reactions for sublimation of the iridium are:



However, previous studies at MIT have found loss of iridium during experiments in LUNAR due to sublimation to be negligible [22]. Furthermore, in this study, chemical analysis of condensates trapped in filters on the exhaust lines of the furnaces have shown no traces of iridium⁶. While the formation of volatile oxides is thermodynamically favorable, it is likely that the oxides would become quickly dissolved in the electrolyte or arrested at the anode surface due to the viscosity of the electrolyte and decompose back into iridium metal by reaction (6) and adsorb back on the anode's surface. However, under varying process parameters, material loss associated with the sublimation of iridium may be accelerated.

⁶ SEM/EDAX found no traces of iridium metal in condensates collected in a cold-trap on the furnace exhaust line during electrolysis with iridium anode in LUNAR electrolyte.

4.1.1 Suggested Experimentation to Quantify Corrosion Rate of Iridium

An unfortunate artifact of MOE studies is the tedious preparation and often tenuous results, which has become increasingly magnified with progressive scale-ups. Therefore, to date, acquisition of large collections of reliable data points has been elusive. A larger set of experiments very similar to those detailed in Chapter 3 could be exceedingly valuable in testing equation 10 and establishing numerical relations between optical basicity, current density, and linear recession rate of iridium. These numerical relations could then be used to engineer parameters such as electrolyte chemistry and operating current density in order to maximize service life of iridium anodes and minimize the costs associated with using the extremely expensive material. During this study it was generally realized that even in the best case scenario, iridium will never be a suitable candidate for iron production by MOE. Therefore, to date, it has been determined that the energy required to develop such numerical models is not warranted at this time. However, such information will likely be very useful if iridium is chosen an anode for further scale-up for lunar production of oxygen or commercial production of high-purity iron. The following paragraphs propose one possible method for empirically verifying the validity of equation (10) and developing a numerical model for the inertness of iridium anodes.

It has been shown that under MOE operating conditions, the reactions given in (4-6) are all thermodynamically favorable and should occur simultaneously. Therefore, developing a numerical model as a function of operating conditions of the separate rate expressions (7), (8), and (9) would be impossible with data from MOE experiments. However, one should be able to design 3 separate sets of experiments to test the kinetics of the 4 reactions, given in (4-6), separately. This would be facilitated by having each set of experiments with conditions such that only one of the reactions given in (4-6) is thermodynamically favorable. Therefore, the effect of the suspected rate-determining parameter on the kinetics of that reaction (e.g. effect of current density on R_{anode}) could be tested. The following three paragraphs details three possible sets of experiments which could theoretically achieve this goal.

Experiment Set 1: Iridium oxide spontaneously decomposes under partial pressures of oxygen

around 1 atm at temperatures above 1300°C [26]. Therefore, one could test the effect of current density alone on rate of iridium oxide formation by performing electrolysis in a highly acidic molten oxide electrolyte with a melting temperature well below 1300°C and that contains no aliovalent cations; a borosilicate glass would fit these criteria. The acidity of the electrolyte would arrest reaction (5). Furthermore, iridium oxide decomposition reactions given in (6) require either high temperatures to make iridium oxide unstable, or cations of aliovalent metals in low oxidation states that can undergo redox reactions with iridium oxide. Therefore, the decomposition reactions given in (6) would also be arrested in these experiments

Experiment Set 2: In these experiments the dissolution rate of iridium oxide in slags of varying optical basicity could be determined by measuring weight loss of iridium oxide pellets submerged in a molten oxide electrolyte for a measured period of time. Since no electrolysis would be performed, reaction (4) would not occur. Furthermore, similar to experiment set 1, one could use a low melting temperature electrolyte with no aliovalent cations to arrest decomposition reactions given in (6).

Experiment Set 3: Finally, one could develop an empirical model for R_{redox} by measuring the extent of decomposition of iridium oxide pellets per unit time when submerged in a highly acidic molten oxide slag as a function of temperature and iron cation concentration. These experiments would be performed without electrolysis and in a highly acidic slag to arrest dissolution of IrO_2 . When the iridium oxide decomposes, it releases oxygen in a gaseous state. Therefore, it would be technically possible to calculate the extent of decomposition by weight loss of the iridium oxide pellet. However, recovering the iridium oxide pellet after the experiment would probably result in entrained electrolyte on the pellet surface, leading to error in the mass measurements. Therefore, a more elegant method to determine the extent of decomposition would be to use a characterization tool that can differentiate between iridium atoms in different oxidation states (e.g. X-ray diffraction or some form of mass spectroscopy). By analyzing the chemical composition of appropriately chosen sample sites within the system, one could integrate over the resulting concentration gradient to evaluate total amount of Ir^0 in the system.

Experiment sets 1 and 2 would be conducted at several hundred degrees Celsius below the

operating temperature of an MOE cell. Therefore, the kinetics of the reactions evaluated with these experiments will likely be much slower than the same reactions during an MOE experiment. As an attempt to overcome this drawback, one could perform experiment sets 1 and 2 at several low temperatures to develop an Arrhenius relationship that could be extrapolated to the MOE temperature regime in order to estimate the kinetics of these reactions during an MOE experiment.

4.2 Anodes with Different Corrosion Mechanisms

In this study iridium has been extensively researched due to its truly unique qualities that allow it to operate as an inert anode for MOE. However, the cost and scarcity of iridium metal will most likely make it an impossible material for use in commercial scale production of iron. Section 3.1.1 details experimental results from tests performed using a graphite anode with a ~1mm iridium coating. While iridium plating would allow an anode to possess the truly unique surface chemistry of iridium for a fraction of the capital costs, it will likely still be far too expensive to use. This study, as well as previous work performed at MIT, have shown that, when used with silicate electrolytes and current densities below 1 A/cm², iridium qualifies as an inert anode by the standard set forth by the aluminum industry (10mm/yr recession rate). However, based on this standard of inertness, if we assume that an industrial MOE cell could produce iron from Fe₂O₃ using iridium anodes at 1 A/cm² current density with 100% current efficiency, the cost of just the anode material lost due to corrosion, based on an average market price of \$23/g for iridium, would be \$521.95 per amp per year, or **\$85,614 per metric ton of iron produced!** Because this is the cost of material lost due to the 10mm/yr recession rate of an inert anode, this cost would be the same for solid iridium anode and plated iridium anodes alike. Therefore, one can quickly realize that iridium will never be a viable anode material for industrial-scale iron production by this standard of inertness. It may be possible that further research, such as that proposed in the previous chapter, could engineer an MOE process in which iridium recession rate is reduced to essentially zero. At that point, iridium coatings or alloys could be considered for iron production. However, it is the author's opinion that the far more elegant solution lies in anodes that do not rely on prohibitively expensive platinum group metals.

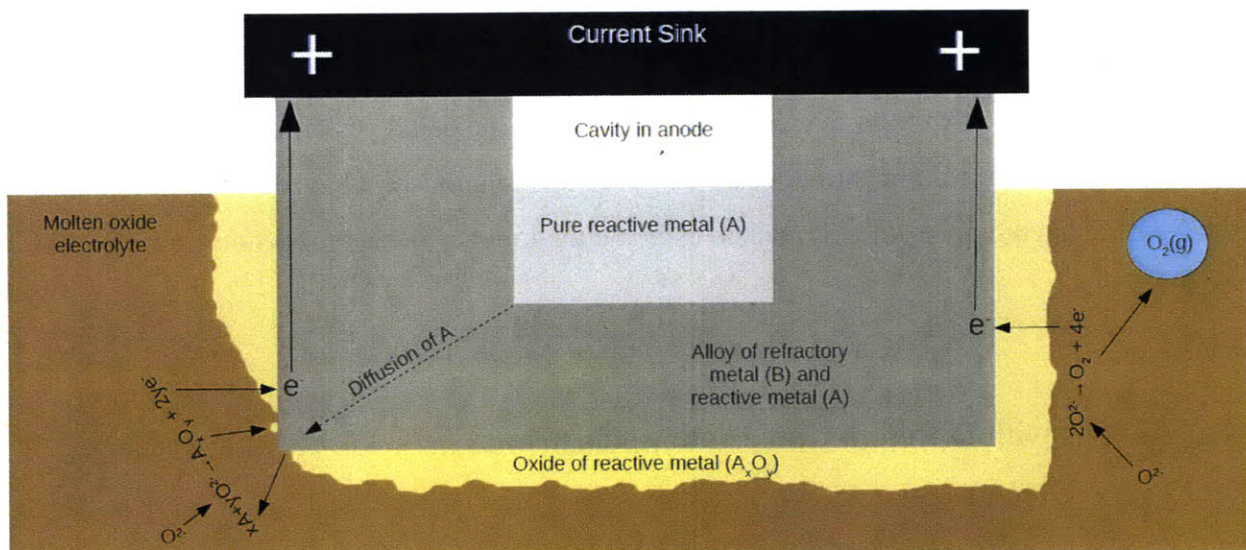


Figure 4.2: Schematic of an oxide-passivated inert anode for molten oxide electrolysis.

Section 1.2.2.2 describes the fundamental concepts behind oxide-passivated inert anodes. Current MOE research at MIT is investigating these materials as the most likely inert anode candidates for iron production. The greatest obstacle that must be overcome is engineering the oxide layer. Ideally, this layer would be impervious to corrosion by the molten oxide electrolyte. However, because the molten oxide electrolyte contains several oxide components, it tends to be an excellent solvent for most oxides. Furthermore, many oxides tend to have large band gaps resulting in very poor electronic conductivity. Therefore, in order for these oxides to work on an MOE anode, they would have to be thin enough ($<1.5\text{nm}$) to allow electron tunneling [14]. Another option would be to use an oxide which is electronically conductive, as this would allow a much thicker oxide coating to be grown on the substrate without creating a dramatic IR drop at the anode. The last important consideration for the oxide coating is the availability and cost associated with using that material, as well as the availability and cost of a compatible refractory substrate.

A very promising candidate for oxide passivation is Cr_2O_3 . Chromium oxide coatings are well known for their excellent corrosion resistance. In fact, Cr_2O_3 coatings are used in the glass industry to withstand even the most corrosive molten oxides [27]. Furthermore, Cr_2O_3 exhibits p-type semi-conduction at MOE operating temperatures [28]. Chromium is relatively inexpensive, meaning even if the oxide is slowly dissolved by the electrolyte, it would still be an

affordable candidate. Plus, if chromium metal did make it into the cathodic product, it could be a welcome “contaminate” by imparting stainless behavior to the iron. However, chromium is also a fairly reactive metal, meaning it will have a higher reduction potential than iron and could be easily prevented from entering the cathodic product. While the results are still very inconclusive, a few preliminary tests in this study with chromium alloys seem to show promising levels of inertness when used as MOE anodes.

Ceria is believed to have excellent dissolution resistance against molten oxides. Additionally, at MOE operating temperatures, doped CeO_2 has been reported to have promising electronic conductivities [29]. While cerium is technically a rare earth metal, it is the most abundant of the rare earth metals. According to a study performed in 1997, cerium is believed to have a crustal abundance of 66.5ppm [30]. Therefore, if a suitable substrate is identified, ceria coatings could be utilized to engineer a promising inert anode material. However, the addition of ceria to silicate glasses has shown to enhance the silicate's electronic conductivity [31]. Since electronic conductivity decreases current efficiency in an electrolysis cell, care must be taken that the ceria coating does not overly contaminate the electrolyte. Furthermore, under certain partial pressures of oxygen at high temperatures, the ceria crystal structure has defect patterns that facilitate oxide ion conductivity. Oxide ion conductivity of the passivation layer could result in unabated growth of the passivation layer, which would cause an unwanted increase in resistance. The first step to determine CeO_2 compatibility with the electrolyte is chemical stability tests; in which a bulk CeO_2 pellet is submerged in the electrolyte and weight loss is used as a means to estimate the recession rate of the theoretical coating. However, preliminary results from these corrosion tests are inclusive.

Magnesium oxide crucibles seem to have excellent resistant to dissolution by silica-free electrolytes with high optical basicity, such as IRON2. Therefore, this oxide has been considered as a widely available and inexpensive candidate. Due to the very reactive nature of magnesium, it is likely that a magnesia coating will preferentially form on the surface of an alloy of magnesium and some refractory. However, magnesium tends to have very poor alloying behavior in nearly all refractory metals [32]. There is a possibility of using titanium as a substrate. At 1600°C , magnesium will form a solid solution with titanium up to 10at% magnesium [33].

However, the fact that titanium is fairly reactive and that magnesium would have fairly low activity in the solid solution, due to its 10at% concentration, might cause some titanium to simultaneously oxidize with the magnesium. It is uncertain whether or not the addition of titanium oxide would affect the resistance of the magnesia layer to dissolution by the electrolyte. There is also the possibility of using an iron oxide-passivated anode. While any of the three iron oxides are susceptible to dissolution by the electrolyte, the addition of iron oxide to the melt would obviously not contaminate the cathodic product. Iron oxides, particularly FeO and Fe₃O₄, have decent electronic conductivities at MOE operating temperatures. This makes them attractive for the oxide passivation layer, but also raises concern. If too much iron oxide is dissolved from the anode surface and into the melt, the resulting spike in electronic conductivity could significantly lower the cell's current efficiency. Iron is not a very reactive metal. Therefore, the substrate would have to be a fairly noble metal with a very high melting temperature. A possible candidate for the substrate would be an inexpensive platinum group metal, ruthenium, which costs about \$6/g in the current market. Fortunately, iron and ruthenium form a solid solution at 1600°C up to approximately 60at% iron [34].

While it would be nominal to identify an oxide impervious to dissolution by the electrolyte to use as the passivation layer, it is a very real probability that no oxide would be able to resist attack by the electrolyte long enough to be classified as truly inert. If this turns out to be true, the anode will have to be continuously regenerating its oxide layer by consuming the reactive metal from the alloyed substrate near the oxide/substrate interface. Therefore, the service life of an oxide-passivated anode will be determined by the depletion rate of the reactive metal in alloyed substrate. This could be a serious concern with systems in which the reactive metal solubility is very low (e.g. Mg/Ti system), or where the dissolution rate of the oxide layer might be fairly fast (e.g. Fe or Cr oxides). An elegant solution to this obstacle is to replenish the concentration of the reactive metal near the substrate/oxide interface by diffusion.

This may be achieved by using a hollow anode. Such an anode would have a cavity in the center of it, in which a supply of the reactive metal could be placed. If the diffusion kinetics are fast enough, there would always be a high concentration of the reactive metal at the substrate/oxide interface. An antecedent to the MOE project at MIT enjoyed success using this concept to design

possible inert anodes for the Hall-Héroult process. It is believed that if a proper reactive metal and suitable substrate are identified, this process should work for MOE. The ability to maintain a desired concentration of reactive metal near the oxide/substrate interface relies on the diffusion kinetics. Therefore, because diffusion rate is a function of temperature, the much hotter MOE process should be able to repeat the success enjoyed with the Hall-Héroult process.

4.3 Cold-Wall Cells for the Next Scale

It has been mentioned several times throughout this manuscript that the maximum length of a laboratory-scale MOE experiment is determined by the life of the crucible. Unfortunately, crucible failure has been the primary contributing factor to data corruption in this project. As the experiments grow in scale, the difficulty of locating suitable materials to contain the highly corrosive electrolyte increases drastically. Therefore, this has limited the scale to which MOE can be tested in a laboratory.

Fortunately, this frustration is purely an artifact of laboratory-scale experimentation. In a working Hall-Héroult cell, the closest industrial equivalent to an MOE cell, the ceramic containment materials are protected by a frozen electrolyte shell that encapsulates the molten cryolite. The formation of this shell is facilitated by the temperature gradient that is inherent to

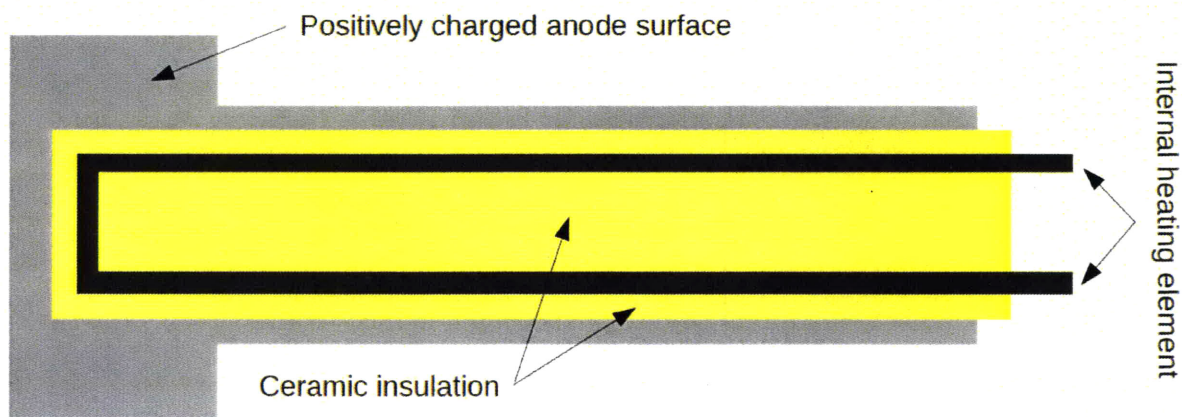


Figure 4.3: Schematic of possible anode design for laboratory-scale, cold-wall MOE cell.

the joule heating mechanism that melts the electrolyte. In a full scale MOE cell, the high temperatures necessary to melt the electrolyte are maintained by joule heating caused by the electrolysis itself. Therefore, the heat emanates from the electrolytically active volume at the center of the cell, causing the extremities to be cooler and, therefore, solidified.

Generating enough joule heating just from electrolysis will require a full-scale MOE cell. This means it will be impossible to design a self-heated, cold-walled cell at the laboratory-scale. Because of this, there is a disconnect between the largest possible laboratory-scale experiments, using current methods, and the smallest self-heated cell. Therefore, in order to evaluate MOE at progressively larger scales will require a new method for heating the electrolyte.

In order to generate the thermal gradient required to cause a frozen shell to form, the cell will have to be heated from the center. The most obvious solution is to heat the anode and cathode, which in turn will heat the electrolytically active volume around the electrodes. The simplest way to achieve this would be to embed resistance heating elements inside the anode and cathode (Figure 4.3). However, the heating elements would have to be on a separate circuit than the electrolysis to prevent disruption of either currents. Therefore, the electrodes would have to be laminated layers of electrically conducting and insulating materials. The largest engineering challenge will be to find the materials and geometries necessary to allow the electrodes to heat up and cool down. An improper design would cause the electrode to break during temperature shifts, due to differences in thermal expansion coefficients of the layers. There are also some far more eloquent designs for achieving a cold-wall cell without joule heating that are under investigation at MIT. However, due to intellectual property concerns, these design cannot be described in this paper.

Chapter 5: Concluding Remarks

Molten oxide electrolysis has the potential to provide a radically new solution to one of the most universal problems facing the world today. Steel is ubiquitous, and has been for generations. The mechanization of industry and birth of the metropolis caused a ravenous demand for iron and steel during the industrial revolution. The incalculable demand for iron caused unprecedented necessity for large scale production and inspired the imagination and brute intelligence of 19th and early 20th century contemporaries. The result was exceedingly ingenious and prolific pyrometallurgical processes to meet the demand - processes that have remained sufficient, in terms of production volumes, throughout the years. The original efficacy of the methods nearly made innovation obsolete from the beginning. However, as demand has sustained and increased throughout the years, the environmental consequences of using carbothermic reduction have begun to have an impact that can no longer be neglected.

The iron and steel industry is one of the largest contributors of greenhouse gas emissions from the manufacturing sector [4]. Great strides have been made by the iron and steel industry to decrease carbon emissions from traditional steel-making. However, the current technologies are incapable of eliminating GHG emissions. The oxidation of carbon and resulting emission of gaseous carbon compounds is intrinsic to the process. Therefore, a radically new technology with fundamentally different chemistry is absolutely necessary for the realization of carbon-neutral, tonnage-scale iron and steel production. Molten oxide electrolysis has been identified by the American Iron & Steel Institute as one of four probable breakthrough technologies to dramatically reduce CO₂ emissions from the iron and steel industry [35].

Molten oxide electrolysis is capable of producing liquid iron metal. However, the ability of the process to do so with zero carbon emissions hinges on the ability to identify an inert anode that fits the criteria listed in section 1.2.2. Laboratory-scale success has been enjoyed with the use of an iridium anode. However, the cost and rarity of the platinum group metal will almost certainly prohibit the development of an iridium anode based MOE cell for industrial-scale iron production. Iridium anodes could be feasible for esoteric applications such as lunar production

of oxygen and commercial production of high-purity iron. However, the implications of developing MOE for those niche demands pale in comparison to the social and environmental significance of revolutionizing the iron and steel industry.

It is unlikely that iridium anodes will ever meet the needs for an industrial process. However, iridium is a very easily obtained and widely available material that can be used at the laboratory scale to facilitate studies on the other intricacies of MOE. Furthermore, understanding the unique corrosion mechanisms that lead to the inertness of iridium as a anode material provides valuable insight into the thermodynamic and kinetic mechanisms of MOE. Additionally, understanding iridium could very well lead to the development of engineered materials, that have yet to be considered, for use as inert anodes. Therefore, regardless of iridium's role in future MOE studies, the data from studying iridium's inertness as a function of electrolyte basicity and current density should prove valuable for future investigations.

In the author's opinion, the most likely candidate for an inert anode for iron production will be an oxide-passivated metal, discussed in sections 1.2.2.2 and 4.2. The temperature gradient and electrochemical requirements of MOE call for the mechanical and electrical properties of metals, while the corrosiveness of the molten oxide electrolyte and highly oxidizing environment of the MOE cell require chemical stability only found in ceramics. A metallic substrate with an oxide coating would meet both of these criteria.

References

- [1] IEA, "ES: Tracking Industrial Energy Use and CO₂ Emissions." OECD/IEA (2007)
- [2] Climate Leaders, "CLIMATE LEADERS GREENHOUSE GAS INVENTORY PROTOCOL, CORE MODULE GUIDANCE: Direct Emissions from Iron & Steel Production." U.S. EPA (2004)
- [3] C. Xu & D. Cang, "A Brief Overview of Low CO₂ Emission Technologies for Iron and Steel Making." *Journal of Iron and Steel Research, International* **17** 1-7 (2010)
- [4] M. Schipper, "Energy-Related Carbon Dioxide Emissions in U.S. Manufacturing." DOE/EIA (2005)
- [5] S. Siitonen, M. Tuomaala & P. Ahtila, "Variables affecting energy efficiency and CO₂ emissions in the steel industry." *Energy Policy* **38** 2477-2485 (2010)
- [6] "Volume 2, Properties and Selection: Nonferrous Alloys and Special-Purpose Materials→Magnetically Soft Materials→Alloy Classifications and Magnetic Testing Methods" in ASM Handbooks Online, ASM International (2002) Accessed: July 1, 2010
- [7] A.H. Sirk, D.R. Sadoway & L. Sibille, "Direct Electrolysis of Molten Lunar Regolith for the Production of Oxygen and Metals on the Moon." *ECS Transactions*, **28** 367-373 (2010)
- [8] A.J. Gmitter, *The Influence of Inert Anode Material and Electrolyte Composition on the Electrochemical Production of Oxygen from Molten Oxides*. Massachusetts Institute of Technology, Cambridge (2008)
- [9] I. Galasiu, R. Talasiu & J. Thonstad. *Inert anodes for aluminium electrolysis*. Aluminium-Verlag Marketing and Kommunikation GmbH, Düsseldorf (2007)
- [10] D.R. Sadoway, "Inert anodes for the Hall-Heroult cell: the ultimate materials challenge." *JOM* **53** 34-35 (2001)
- [11] T. Akai, J. Nishii, M. Yamashita & H. Yamanaka, "Chemical behavior of platinum-group metals in oxide glasses." *Journal of Non-Crystalline Solids*, **222** 304-309 (1997)
- [12] G.D. Smith & E. Zysk. "Volume 13, Corrosion: Corrosion of the Noble Metals." in ASM Handbooks Online, ASM International (2002) Accessed: July 1, 2010
- [13] N. Pilling & R. Bedworth, "The oxidation of metals at high temperatures." *J. Inst. Metals* **29** 529-582 (1923)

- [14] A.J. Bard & L. R. Faulkner. *Electrochemical methods : fundamentals and applications* - 2nd Edition. D. Harris, E. Swain, C. Robey & E. Aiello (Eds.). John Wiley & Sons, Inc (2001)
- [15] E. Olsen & J. Thonstad, "Nickel ferrite as inert anodes in aluminium electrolysis: Part I Material fabrication and preliminary testing." *Journal of Applied Electrochemistry* **29** 293-299 (1999)
- [16] C.F. Windisch, D.M. Strachan, C.H. Henager, E.N. Greenwell & T. R. Alcorn, "Results From a Pilot Cell Test of Cermet Anodes. Inert Electrodes Program ." *Gov. Res. Announc. Index* 209.17 (1992)
- [17] *Slag Atlas* - 2nd Edition. Verein Deutscher Eisenhüttenleute (VDEh) (Ed.). Verlag Stahleisen GmbH, Düsseldorf (1995)
- [18] FactSage, Ver. 6.1, Thermfact & GTT-Technologies
- [19] G. Ottonello & R. Moretti, "Lux-Flood basicity of binary silicate melts." *Journal of Physics and Chemistry of Solids* **65** 1609-1614 (2004)
- [20] J.A. Duffy, "A review of optical basicity and its applications to oxidic systems." *Geochim. Cosmochim. Acta* **57** 3961-3970 (1993)
- [21] B. Sessink & N. Verster, "Design of elastomer O-ring vacuum seals." *Vacuum* **23** 319-325 (1973)
- [22] D. Wang, A.J. Gmitter & D. R. Sadoway, "An inert anode for the production of oxygen gas by electrochemical decomposition of an oxide melt." Unpublished.
- [23] L. Bozza. "Volume 2: Properties and Selection→Nonferrous Alloys and Special Purpose Materials→Pure Metals→Properties of Pure Metals→Iridium." in ASM Handbooks Online, LToth (Ed.) ASM International (2002) Accessed: July 10, 2010
- [24] R.A. Watson, B. Jönsson, G.A. Fielding, D.V. Cunningham & C. D. Starr. "Volume 2: Properties and Selection→Nonferrous Alloys and Special Purpose Materials→Special Purpose Materials→Electrical Resistance Alloys→Properties of Electrical Resistance Alloys→Molybdenum Disilicide." in ASM Handbooks Online, ASM International (2002) Accessed: July 15, 2010
- [25] HSC Database, Vers. 5.11, Outokumpu
- [26] K.T. Jacob, T.H. Okabe, T. Uda & Y. Waseda, "Solid-State Cells with Buffer Electrodes for the Measurement of Thermodynamic Properties of IrO₂, CaIrO₃, Ca₂IrO₄, and Ca₄IrO₆." *Journal of The Electrochemical Society* **146** 1854-1861 (1999)

- [27] "Engineered Materials Handbook→Traditional Applications for Ceramics→Refractories." in ASM Handbooks Online, ASM International (2002) Accessed: July 1, 2010
- [28] D.M. Smyth, "Electrical Conductivity of Ceramic Materials", in *Advanced Ceramics*. 147-164, S. Saito (Ed.) Oxford University Press, Oxford (1988)
- [29] V.V. Kharton & F. M. B. Marques, "Mixed ionic-electronic conductors: effects of ceramic microstructure on transport properties." *Current Opinion in Solid State and Materials Science* **6** 261-269 (2002)
- [30] C.K. Gupta & N. Krishnamurthy. *Extractive Metallurgy of Rare Earths*. CRC Press (2004)
- [31] V. Deshpande & R. N. Taikar, "Effect of cerium oxide addition on electrical and physical properties of alkali borosilicate glasses." *Materials Science and Engineering: B* **172** 6-8 (2010)
- [32] M. Pekguleryuz & M. Avedesian, "Magnesium alloying- Some potentials for alloy development." *Japan Institute of Light Metals, Journal* (1992)
- [33] J.L. Murray, "Mg-Ti Phase Diagram." in ASM Alloy Phase Diagrams Center, ASM International (1990) Accessed: August 1, 2010
- [34] L.J. Swartzendruber & B. Sundman, "Fe-Ru Phase Diagram." in ASM Alloy Phase Diagrams Center, ASM International (1990) Accessed: August 1, 2010
- [35] AISI, "CO2 Breakthrough Fact Sheets." <http://www.steel.org/AM/Template.cfm?Section=Fact_Sheets2&TEMPLATE=/CM/HTMLDisplay.cfm&CONTENTID=18071> Accessed: August 1, 2010